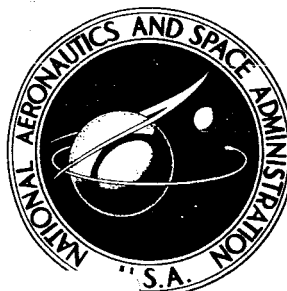


# NASA CONTRACTOR REPORT



NASA CR-251

NASA CR-251

FACILITY FORM 602

N65-27820

(ACCESSION NUMBER)	(THRU)
64	1
(PAGES)	(CODE)
	06
(NASA CR OR TMX OR AD NUMBER)	(CATEGORY)

GPO PRICE \$  
01-571  
OTS PRICE(S) \$ 3.00

Hard copy (HC)

Microfiche (MF) 55

## STUDY OF THE GROWTH PARAMETERS INVOLVED IN SYNTHESIZING BORON CARBIDE FILAMENTS

by A. Gatti, C. Mancuso, E. Feingold,  
R. Mehan, and R. Cree

Prepared under Contract No. NASw-937 by  
GENERAL ELECTRIC COMPANY  
Philadelphia, Pa.  
for

STUDY OF THE GROWTH PARAMETERS INVOLVED IN  
SYNTHESIZING BORON CARBIDE FILAMENTS

By A. Gatti, C. Mancuso, E. Feingold,  
R. Mehan, and R. Cree

Distribution of this report is provided in the interest of  
information exchange. Responsibility for the contents  
resides in the author or organization that prepared it.

Prepared under Contract No. NASw-937 by  
GENERAL ELECTRIC COMPANY  
Philadelphia, Pa.

for

NATIONAL AERONAUTICS AND SPACE ADMINISTRATION

## TABLE OF CONTENTS

<u>Section</u>	<u>Page</u>
I SUMMARY	1
II INTRODUCTION	2
A. OBJECTIVES AND APPROACHES	2
1. Growth	2
2. Strength	3
3. Structure	3
4. Composite Studies	3
III EXPERIMENTAL PROCEDURES AND RESULTS	5
A. GROWTH STUDIES	5
1. Description of Equipment	5
2. Catalytic Studies	6
3. Geometric Conditions Affecting Growth	7
4. The Dynamic Method	9
5. Boron Additions	10
B. MECHANICAL PROPERTIES OF $B_4C$ WHISKERS	11
C. CRYSTAL AND MORPHOLOGICAL CHARACTER OF $B_4C$ WHISKERS	12
1. Experimental Methods and Techniques	13
a. Optical Microscopy	13
b. Electron Microscopy	13
(1) Direct Transmission EM	13
(2) Replication EM	13
(3) X-Ray Diffraction	15
(4) Electron Diffraction	15
2. Discussion and Results	15
a. Surface Character (Topography)	15
b. Origin of Characteristic Topography	16
c. Crystal Character and Whisker Orientation	19
d. Whisker Termini	20
3. Mechanism of $B_4C$ Whisker Growth	21

## TABLE OF CONTENTS (Cont'd)

<u>Section</u>	<u>Page</u>
D. COMPOSITE STUDIES	22
1. Impregnation Techniques	22
2. Fernico "5" Composites	24
3. PJ 122 Composites	25
4. Aluminum Composites	25
IV CONCLUSIONS	28
ACKNOWLEDGEMENTS	31
REFERENCES	32
FIGURES	



## LIST OF FIGURES

### Figure

1. Photograph showing the effect of vanadium on the growth of  $B_4C$  whiskers. Of the two growth tubes shown, vanadium was added to the charge only in the furnace containing the lower tube
2. Photograph showing additional mandrel added to top of "lazy susan" tray (about 1/3 size)
3.
  - a. Typical run before the internal mandrel and baffle additions (about 1/2 size)
  - b. Typical run after mandrel and baffle additions (about 1/2 size)
4.
  - a. Schematic representation of proposed conical chimney design
  - b. Schematic representation of hypothesized vapor gradient
5. Schematic design of whisker bend-test apparatus
6. Load-deflection calibration curve of .001 diameter tungsten wire at room temperature
7. Photograph at 1/3 size of tube-capillary and arrangement for epoxy impregnation of  $B_4C$  whisker bundles
8. Schematic diagram of furnace for fabricating  $B_4C$ -metal composites by pneumatic pressure technique
9. Preparation of primary cellulose acetate replica of a small object
10. Schematic representation of typical topographical details observed on  $B_4C$  whiskers
11.  $B_4C$  whisker surface details. Magnification = 875X
12.  $B_4C$  whisker surface details. A. Note large scale imperfections near whisker tip. Magnification = 875X
13. Electron photomicrograph of a replicated portion of a "smooth"  $B_4C$  whisker. Magnification = 25,200X

## LIST OF FIGURES (Cont'd)

### Figure

14. Electron photomicrographs of portions of "smooth"  $B_4C$  whiskers. Magnification = 20,000X
15. Transmission electron photomicrograph of a thin  $B_4C$  whisker. Note the stacking fault configurations parallel to  $\vec{a}_1$  and  $\vec{a}_2$ . Magnification = 69,000X
16. Transmission Electron photomicrograph of a thin, cylindrically bent  $B_4C$  whisker. Note stacking fault configuration parallel to  $\vec{a}_1$  (arrows) and parallel to  $\vec{a}_2$ . Magnification = 30,000X.
17. Transmission electron photomicrograph of a thin  $B_4C$  whisker. Note symmetry about AA and  $\vec{a}_1$ . Magnification = 36,000X
18. Typical, but rare, outgrowths from  $B_4C$  whiskers. Magnification = 875X
19. Transmission electron photomicrograph of a  $B_4C$  whisker during a late stage of development. Magnification = 30,000X
20. Transmission electron photomicrograph of a region of a typical  $B_4C$  whisker (a) and an electron diffraction pattern of the same region (b).
21. X-ray diffraction "Layer Line" photograph (2.2X) of a typical ("a" type)  $B_4C$  whisker. The whisker axis was parallel to  $a$ .
22. Predicted quadrilateral whisker cross sections
23. Flag or pennant tip of maturing  $B_4C$  whisker transmission electron photomicrograph. Magnification = 30,400X
24. A. Field of  $B_4C$  whiskers, on their growth mandrel, showing flags or pennants on their tips, Magnification = 163X  
B. Pennanted tip of a  $B_4C$  whisker. Pennant is directed toward observer. Magnification = 875X

## LIST OF FIGURES (Cont'd)

### Figure

25. Flag region of  $B_4C$  whisker electron photomicrograph of replica. Magnification = 20,000X
26. Schematic representation of factors involved in  $B_4C$  whisker growth process

## I. SUMMARY

The present program is a continuation of a study sponsored by NASA on Contract NASw-670. The current program is concerned with (1) the synthesis of boron carbide whiskers, (2) the characterization of these whiskers in terms of their chemical and physical properties at room and elevated temperatures, and (3) the utilization of such whiskers in composites.

In addition to the routine runs which provided a supply of  $B_4C$  whiskers for further studies, considerable emphasis was placed on a search for an effective catalyst which would markedly increase both the quantity and the size of  $B_4C$  whiskers grown. It was found that vanadium serves as the best catalyst in this respect although the elements which occur in proximity to vanadium in the periodic table, namely, molybdenum and niobium, are also effective.

Since the surface perfection of the micro-crystals play an important role in determining their strength, studies on surface morphology of  $B_4C$  whiskers were included. A significant observation was that no overgrowths occur on the whiskers. However, surface defects do exist on all whiskers when studied at high magnifications. Also, evidence is presented which shows that a highly saturated vapor exists in the  $B_4C$  whisker deposition areas.

Several tensile tests of the  $B_4C$  whiskers were performed previously at room temperature in order to determine their strengths and strength distribution. Thus far, from a total of twenty tests, tensile values varied from a low of 179,000 psi to a high of 965,000 psi with an average value of 400,000 psi. Elevated temperature tests are presently being attempted. A description of the technique to be used and the problems yet to be solved are presented.

A series of studies were performed in an attempt to produce composites of epoxy- $B_4C$ , aluminum- $B_4C$ , and an Fe-Ni-Co alloy- $B_4C$  by liquid infiltration of the matrix. Room temperature tensile tests on  $B_4C$ -aluminum composites have shown values as high as 29,500 psi. A discussion of the progress made in composite formation is presented.

## II. INTRODUCTION

In a previous study<sup>(1)</sup>, whiskers of  $B_4C$  were synthesized for the first time so that their crystalline and mechanical properties could be determined. In addition, preliminary studies were undertaken for the purpose of evaluating composite materials containing  $B_4C$  whiskers. The results of this study have shown that  $B_4C$  crystals possess an excellent combination of physical properties, in terms of high elastic modulus, high strength, and low density. Thus, these whiskers as reinforcements offer one of the greatest potentials for high strength-to-weight or high stiffness-to-weight materials of the future. In addition, the refractory properties of the  $B_4C$  whiskers make them a prime candidate for reinforcing materials at high temperatures.

The present investigation is a continuation of this study, with special emphasis being placed on (1) the scale-up of  $B_4C$  whisker production, on (2) the testing of individual whiskers at elevated temperatures, and on (3) the fabrication and testing of composites containing these whiskers.

### A. OBJECTIVES AND APPROACHES

#### 1. Growth

An extensive study was made previously<sup>(1)</sup> on the growth parameters which could affect the production of  $B_4C$  whiskers. Two basically different methods were studied. The pure-vapor method which involves the vaporization of  $B_4C$  at high temperatures and subsequent condensation to  $B_4C$  whiskers, and the dynamic method which attempts to form  $B_4C$  whiskers as a consequence of reacting  $CH_4$ ,  $BCl_3$ , and  $H_2$  also at high temperatures. Further growth studies were initiated during this contract with major emphasis being placed on increasing the quantity and quality of  $B_4C$  whiskers. The pure vapor-method parameters; such as temperature, catalytic effects, and deposition geometry, have been optimized so that many more whiskers have been grown per run than previously. Also, further work on the dynamic method was discontinued because of the dynamic gas conditions which cannot be solved with present furnace designs.

## 2. Strength

It was hoped that strength measurements at high temperatures on individual  $B_4C$  whiskers could have been completed during the present contract period. However, initial studies indicated that numerous modifications of equipment were necessary for having a workable system built. The present system is a unique arrangement which can test very small crystals in bending at high temperatures. A description of the equipment and preliminary calibrating data is presented in this report.

## 3. Structure

Although the orientation and growth habits of  $B_4C$  whiskers were studied previously<sup>(1)</sup>, the present investigation has extended this work with most of the emphasis on understanding the state of crystalline perfection of the as-grown  $B_4C$  whiskers. Since whisker-like crystals derive their excellent mechanical properties from a high degree of crystalline perfection, this study is an important phase of the program.

## 4. Composite Studies

One of the ultimate goals of this study is the effective utilization of  $B_4C$  whiskers as reinforcements in composite materials. Initial work<sup>(1)</sup> had determined that reinforcement of epoxy type resins was possible. Sessile drop experiments have shown that an Fe-Co-Ni alloy (Fernico "5") would wet  $B_4C$  and thus presumably form an excellent bond with  $B_4C$  whiskers. Also the alloy is a suitable matrix for high temperature composite materials studies. Forming composites with a Fernico "5" matrix have proved, however, to be difficult. A number of composites containing  $B_4C$  whiskers in epoxy resin, and aluminum have been fabricated and tested. Attempts have also been made to form composites with a higher temperature matrix. A method has been developed which holds promise for producing excellent composites without the limitations presently imposed by infiltration techniques.

Aluminum matrix composites were fabricated during this contract period. Most of the emphasis was devoted to the development of fabrication

techniques. A few composites were produced for conducting tensile tests. The infiltration technique for forming composites has been used exclusively and is discussed in detail. Limitations of the method are described with recommendations for future work.

In summary, the present effort has further extended the knowledge of  $B_4C$  whisker technology. Growth studies have led to a marked increase in whisker yield as well as a noticeable improvement in their quality. A system has been devised which can measure the high temperature mechanical properties of individual  $B_4C$  whiskers. An extensive study on the perfection of the as-grown  $B_4C$  whiskers has been completed.

### III. EXPERIMENTAL PROCEDURES AND RESULTS

#### A. GROWTH STUDIES

Three techniques were developed previously for growing  $B_4C$  whiskers, and these are described as follows: (1) The pure-vapor method, in which a charge of powdered  $B_4C$  is heated in a "lazy Susan" type tray in order to enhance the vaporization of pure  $B_4C$ . Whiskers of  $B_4C$  are then formed in a cooler region of the furnace, (2) The dynamic method, which consists of controlling the flow of the individual gases which react to form  $B_4C$  as they flow through a smaller furnace containing two variable hot zones, and (3) A combination of methods (1) and (2) which utilizes a carrier gas flowing over a "lazy susan" charge of pure  $B_4C$  powders in a small two-zoned furnace.

The present growth studies were concerned with increasing the whisker yield to provide whiskers for composite fabrication. Emphasis was placed on utilizing the pure vapor method, on developing an effective catalyst which would control the size and population of  $B_4C$  whiskers, on geometric considerations which effect growth conditions, on a final evaluation of the dynamic method, and on a study to determine if boron itself could be used as a starting material to produce whiskers.

##### 1. Description of Equipment

Growth studies were performed in graphite resistance furnaces which were described previously<sup>(1)</sup>. Experiments based on the pure-vapor technique were performed in the large furnace which has a 54" dia. x 10" long hot zone capable of reaching 2200°C in a 50μ vacuum. Dynamic experiments were performed in the smaller stacked furnace containing two 1 inch dia. x 6 inch long independently controlled hot zones and capable of operating to 2000°C in a 50μ vacuum. Modifications were made in the deposition zone of the large furnace as a result of the studies of geometric conditions which affect whisker growth and populations and are described in section A-3 of this report.



## 2. Catalytic Studies

The effect of a catalytic impurity was suspected in the earlier growth studies, since it was observed that a continued use of the same  $B_4C$  supply in the pure vapor method led to a decrease in the population and in the length of  $B_4C$  whiskers produced. Five or six reruns were sufficient to reduce growth to essentially zero. Indeed, various batches of  $B_4C$  powders were observed to produce notable differences in the length and in the number of whiskers grown. Semi-quantitative spectrographic analysis were obtained of two lots of  $B_4C$  powder as received and after being used in furnace runs to produce whiskers. It was found that a large number of impurities were present before reaction, namely (in decreasing amounts): Fe, Al, Ca, Si, Cr, Ni, Cu, Mn, Ti, W, V, and Mg. After whisker growth, Fe, Ti, Cu, and Si remained in detectable quantities. It was first thought that one or more of these elements remaining after reaction would be effective in promoting whisker growth, and further, that the gradual decrease in whisker population was a direct result of the decreasing concentration of one or more of these elements. Experiments were performed, therefore, in which the elements Fe, Ti, Cu, and Si were added purposely to exhausted  $B_4C$  charges which would no longer produce whiskers.

Analyzing the whiskers themselves by x-ray fluorescence indicated that a trace amount of vanadium was present. Hence, an experiment similar to that previously described was performed utilizing an exhausted charge of  $B_4C$  powder mixed with 1 wt. % vanadium metal powder. A standard run of  $1950^{\circ}C$  for 5 hours was performed and the result was a rejuvenation of  $B_4C$  whisker growth from the formerly exhausted powder. Additional experiments have since been performed to confirm this finding. The growth of whiskers obtained by the addition of V to exhausted  $B_4C$  powder is equal to the best whisker growths obtained with fresh powder. The effect of the vadium addition can be clearly seen in Figure 1, where the upper tube shows no appreciable whisker growth from exhausted  $B_4C$  powder, while the lower tube shows a notable growth of whiskers after vanadium had been added to the charge.

Continuing efforts to determine the catalytic effect of metal vapors on the growth of boron carbide whiskers have been made. Experiments generally consisted of first exhausting the inherent catalyst (viz., vanadium) which is present in the as received boron carbide powder, and then placing the metal powders to be studied in small (1-2 gm total) quantities on all the trays of the lazy-susan.

To date the addition of vanadium, molybdenum, and niobium have increased the production of whiskers from exhausted boron carbide powder. Other metals which have been tried and were unsuccessful include chromium, titanium, and zirconium. These elements were selected because of their proximity to vanadium on the periodic table.

### 3. Geometric Conditions Affecting Growth

A major effort was devoted to the optimization of the various parameters which can influence the growth of  $B_4C$  whiskers so that greater yields of high strength whiskers can be produced. The catalytic effect of vanadium, molybdenum, niobium, and possibly other metal vapors on the growth of  $B_4C$  whiskers was one approach.

Another approach, the geometry of the whisker growth area, was also studied during this reporting period. Since most geometric conditions can affect either the chemical gradient of the vapor available for deposition or the supersaturation of the vapor itself, this geometric parameter is an important variable which deserves consideration.

It was assumed that vapor species present in the deposition area were essentially under molecular flow conditions due to the operating pressure (about 50 microns vacuum). Thus, the deposition mandrel surface was influencing a hollow cylinder-like volume of active vapor, which was about 1-1/2" in outside diameter (the I. D. of the mandrel itself) by about 1 cm in depth as evidenced by whisker lengths produced. The core-volume of vapor (about 1 inch in diameter) was essentially being pumped out of the system and wasted. It was decided to attach an additional deposition surface to the "Lazy Susan" tray arrangement in order to possibly utilize this center portion of vapor which was escaping. Figure (2) shows how such an

attachment was made. The additional mandrel (a) is a hollow graphite can one-half inch in diameter and four inches long with a 11/16 hole drilled into the bottom as a mounting device for fastening the mandrel to the center rod of the "Lazy Susan". The mandrel was purposely hollowed out in order to minimize any effect on the temperature gradient originally present. An improvement in both the number and the quality of  $B_4C$  whiskers was noted. One additional modification was then made. It was further deduced that a baffle above the deposition zone would locally decrease the pumping rate and thereby effectively increase the supersaturation of vapor at the deposition site. The baffle, which was in the form of a graphite disc 1/8" thick of sufficient diameter to slide through the deposition tube (approx. 1-1/2" dia.) perforated with four 1/4" holes, was placed in the deposition mandrel. The top of the center hollow mandrel held the baffle in position. This geometric configuration resulted in a ten-fold increase in yield of  $B_4C$  whiskers. The average length of the whisker product was also increased. Figure 3 illustrates these results. Photograph (a) depicts a typical run before an internal mandrel and baffle, while Photograph (b) shows a typical run with the internal mandrel and baffle added. It can be seen that the growth area has been expanded to include nearly all available deposition surfaces, which is about 4" in length compared to about 1" in the former arrangement.

Several other geometric changes in the deposition zone were made in an attempt to further optimize this parameter. Changes included the internal mandrel length and the deposition mandrel design.

Internal mandrel lengths of five, six, and seven inches were tried but no improvement over the original four inch mandrel was noted. The deposition chimney geometry was changed so that one inch of the chimney protruded down into the hot zone in an attempt to deposit whiskers further down into the furnace. No whiskers were deposited on the extended section although  $B_4C$  was trapped on the outside surface. In a subsequent run, this section was slotted to furnish an easy path for the vapor to impinge on the inner surfaces of the extended mandrel. No benefit was derived from any of the modifications tried thus far.

Further modifications are contemplated since evidence from observations of growth patterns of the  $B_4C$  whiskers and electron microscopic studies of whiskers indicate that a region of highly saturated vapor exists in the deposition zone. This volume of vapor is now essentially being wasted because it does not contribute to axial growth of existing whiskers but is expended by excessive nucleation and dendrite growth on the sides of the originally nucleated whiskers (see Section C of this report). It is envisioned that conically shaped surfaces shown schematically in Figure 4 could redistribute the present gradients of vapor more favorably and decrease the excess concentration which is now occurring. Included in Figure 4 is a representation of the estimated vapor gradients occurring due to the deposition zone geometry now being used.

#### 4. The Dynamic Method

The dynamic growth method produced  $B_4C$  whiskers in situ from the gas phase according to the reaction:  $4BCl_3 + CH_4 + 4H_2 \rightarrow B_4C + 12HCl$ . This method yielded only poorly developed whiskers. The addition of vanadium to this system was also studied by heating  $BCl_3$ ,  $CH_4$ , and  $H_2$  to temperatures of  $1650^\circ C$  for 5 hours with  $VCl_4$  vapor added. A band of well defined  $B_4C$  whiskers were produced in the furnace tube.

Continued efforts failed to improve the quantity or quality of the whisker product. An experiment was performed using pure vanadium by placing small amounts of the metal on each tray of a lazy-susan but no improvement in whisker quantity was noted. It is believed that this method is not practical under present conditions of equipment design for the following reasons.

In the pure vapor experiment the vapor is hot before it passes into the deposition zone of the furnace. In the case of the dynamic system, the gas species passes through a temperature gradient from ambient to the furnace temperature, and a premature reaction in the vapor phase causes a depletion of available boron carbide as it travels through the furnace. The  $B_4C$  depletion is readily seen as a gross deposit in close proximity to the

inlet nozzle of the furnace. Thus, only minute quantities of  $B_4C$  vapor reach the deposition zone, which seriously restricts growth. Premature reaction of the gaseous species could possibly be avoided by major design changes in the nozzle area. However, such revisions would involve complete rebuilding of the present furnace with no guarantee of success. Also, the disadvantage of extraneous gaseous byproducts such as HCl in the growth zone must be considered, since experience has shown that good quality whiskers have not yet been produced under these conditions. No future work on the dynamic method is planned.

#### 5. Boron Additions

The vaporization of  $B_4C$  at various temperatures has been studied by Robins and Gilles<sup>(2)</sup> and others. Their data suggests that  $B_4C$  is not vaporized directly but is transported as elemental boron with at least three intermediate species  $BC_2$ ,  $B_2C$ , and  $B_2$ . The intermediate species vapor is estimated to amount to about 5% of the total, with the bulk of the vapor composition consisting of elemental boron. Thus it would appear that boron is preferentially evaporated from  $B_4C$  with little carbon available in the gas phase for  $B_4C$  reformation once condensation takes place. It could be postulated then<sup>(3)</sup> that  $B_4C$  whisker growth actually takes place by the vapor transport of boron and subsequent reaction with hot graphite furnace parts to  $B_4C$  upon condensation. Definitive experiments to establish such a mechanism are of course impossible in the graphite furnace presently being used. However, observations of the growth behavior of  $B_4C$  whiskers using boron powder as a starting-material can indicate the pertinent transport mechanisms that are occurring.

Accordingly, boron powder (instead of boron carbide powder) was placed on the lazy susan tray and a standard whisker run was made. No whiskers were produced although  $B_4C$  powder\* was formed on the deposition surfaces which would normally be covered with  $B_4C$  whiskers. The run was repeated with vanadium addition and produced similar results. The

---

\* As analyzed by x-ray techniques.

latter tray was again used without re-changing with a fresh supply of boron and stubby crystalline whiskers were produced. X-ray examination of the powder charge and crystals produced confirmed that they were both  $B_4C$ . It is apparent, then, that the original boron charge had all reacted with the graphite furnace parts to form  $B_4C$  in situ after the second treatment.

Thus far, the experiments indicate that  $B_4C$  whiskers cannot be grown under these conditions with elemental boron powder even though boron vapor is the major species evaporated from  $B_4C$ . Either the majority of whiskers are formed by recombination of the carbon bearing species with excess boron to form  $B_4C$  or the evaporation characteristics of  $B_4C$  under conditions used here are such that B and C vapor are always present in sufficient quantity to form  $B_4C$  at the deposition area. The pure boron experiments tend to bear out the latter hypothesis since only  $B_4C$  powder was formed when there was certainly an excess of boron vapor in the system.

#### B. MECHANICAL PROPERTIES OF $B_4C$ WHISKERS

An apparatus has been designed, built, and calibrated at room temperature for conducting bend tests on short lengths of fine filaments at both room and elevated temperatures. The equipment is a modification of the type used by Pearson, Read, and Feldman<sup>(4)</sup>, and is shown schematically in Figure 5. The specimen is supported on a notched ceramic tube positioned over the cross-head of an Instron tensile machine. A quartz filament with a hook on the end applies the load to the specimen through a strain-gaged cantilever-spring load cell mounted on the movable cross-head of the Instron. A Gaertner telescope is independently mounted on the machine frame to measure the specimen deflection (by the vertical displacement of the quartz rod). A micro-furnace has been constructed with fits over the ceramic support tube to conduct tests at elevated temperatures. Calibration tests have indicated that the cantilever load cell is linear between 5 mg and at least 2.0 gms. The deflection measuring system is accurate to about 0.0012 mm and has unlimited travel.

Figure 6 shows typical data obtained on 0.001" dia. tungsten wire run as a check on the instrumentation. The elastic modulus is within 10% of published values ( $5 \times 10^6$  psi) and the elastic and plastic portions of the load-deflection curve are clearly distinguishable. These tests have been repeated about three times, with the moduli falling within 10% of each other.

Preliminary attempts to test  $B_4C$  whiskers have not been successful, even at room temperature. The whiskers available exhibited considerable taper and were too small in effective diameter for the span length used (0.067 inches). The combination of these circumstances lead to immediate pull-out upon attaching the quartz rod. Conway<sup>(5)</sup> has shown that, for the present geometry, the following inequality must hold to avoid non-linear elastic behavior and (eventually) unrestrained deflections leading to pull-out:

$$\frac{\sigma}{E} \frac{l}{d} \leq 0.5 \quad (1)$$

where

- $\sigma$  = stress level
- $E$  = elastic modulus
- $l$  = span length
- $d$  = specimen dia.

Using typical values of  $\sigma$  and  $E$ , and a span length of 0.067", it is found that the diameter must be greater than about  $50\mu$ . Subsequent tests will be performed either on large diameter whiskers or, conversely, will utilize a shorter span length.

#### C. CRYSTAL AND MORPHOLOGICAL CHARACTER OF $B_4C$ WHISKERS

It has been suggested that filamentary crystals or whiskers derive their excellent mechanical properties from their lack of bulk imperfections, lack of mobile dislocations, and from their surface perfection. Their high degree of bulk perfection can be attributed to these facts: (a) they are small and hence cannot accommodate a large number of imperfections; and (b) that the low (vapor) supersaturation conditions which are employed during the growth process permit atomic arrangement to proceed without

numerable accidents. Surface perfection arises from controlled growth conditions which essentially prohibit spurious nucleation and hence prevent spurious overgrowths from occurring on the surface of the maturing whisker.

The work which will be described in this section was done in order to (a) gain a better understanding of growth processes, (b) to elucidate the nature of surface and bulk perfection and (c) to examine growth habits.

### 1. Experimental Methods and Techniques

Optical microscope, electron microscope, x-ray and electron diffraction analyses were made.

#### a. Optical Microscopy

Conventional reflection microscopy methods were used. Examinations were made on a metallographic (inverted) microscope, and the whiskers were held on a glass slide faced with double sided Scotch tape.

#### b. Electron Microscopy

##### (1) Direct Transmission EM

Many very thin (ca.  $1000\text{\AA}$  thick) whiskers were obtained on standard 200 mesh microscope specimen screens by simply passing the screens, which had been pretreated with a suitable\* adhesive, through a field of whiskers on the growth mandrel.

##### (2) Replication EM

A technique for producing surface replicas of particles and fibers of small dimensions was developed<sup>(7)</sup>. An important advantage of the replication method lies in the fact that any particle or fiber that can be handled or manipulated, and is compatible with acetone and cellulose acetate, can be replicated in any desired orientation in any position on a conventional electron microscope specimen screen. The method is described in the following four steps (a-d) .

(a) A standard microscope specimen screen (e.g. 200 mesh) is prepared by: first dipping in acetone and then placing, while wet, on a thin (ca. 0.003 inch) sheet of cellulose acetate which has previously been

---

\*A very satisfactory adhesive for this application can be obtained from Ernest F. Fullam, Inc., Schenectady, N. Y. (Item No. 1137, 1964 catalog)



stretched and taped (scotch tape) to a glass microscope slide, Figure 9A. A drop of acetone is then applied to the back of the specimen screen, Figure 9B. After 10-15 minutes, the acetate film in which the screen is now firmly embedded is carefully stripped from the glass slide. A thin continuous cellulose acetate film will be found to cover the bottom of the specimen grid, Figure 9C. The acetate film containing the grid is next turned over and taped to a clean glass microscope slide, Figure 9D. It may be noted that several screens may be prepared simultaneously.

(b) The specimen(s) of interest is next carefully positioned using tweezers, micro manipulators, etc., over desired openings in the specimen screen, Figure 9E. The small specimens so positioned will be found to be held sufficiently firmly in place, through electrostatic attraction, to enable one to turn the screen, specimen, slide and acetate film over without altering the orientation of the specimen on the screen.

(c) The assembly with the screen and specimen directed down, is then held over a small container of acetone which has been heated to  $50^{\circ}\text{C}$  to  $60^{\circ}\text{C}$ , Figure 9F. The acetone vapor softens the cellulose acetate film. When the film reaches the proper viscosity and surface tension, the specimen will become partially embedded. At this time the assembly is removed from the acetone vapor and the acetate film is permitted to set (approximately 15 minutes). The time required for the acetone vapor to interact sufficiently with the acetate film to obtain the proper conditions of surface tension and viscosity which will ensure "good replication" can be ascertained by making one or two trial runs on a "typical" specimen (20 to 30 seconds is generally sufficient).

(d) The specimen(s) is next pulled (stripped) from the cellulose acetate replica using scotch tape, Figure 9G. After this, conventional methods of replica preparation are used, viz., platinum shadowing, carbon deposition, dissolution of cellulose acetate in acetone, and drying of the replica. It has been found that removal of cellulose acetate can best be accomplished, with least strain on the shadowed carbon replica, through the use of an

appropriate extraction apparatus. The specimen may be reclaimed from the scotch tape by either mechanical means or through the use of solvents. In the following sections, electron photomicrographs of surface replicas which had been prepared from the surfaces of  $B_4C$  whiskers using the above replication method will be discussed. (The reader is referred to Figures 13, 14, and 25).

### (3) X-Ray Diffraction

Single crystal rotation, or layer-line diffraction photographs were obtained from individually mounted  $B_4C$  whiskers. The whiskers were mounted on a goniometer head in a cylindrical, 57.3 mm diameter, x-ray diffraction camera. Nickel filtered copper radiation was used.

### (4) Electron Diffraction

Selected area and transmission electron diffraction examinations were made on sufficiently thin whiskers which were obtained and mounted in the manner described in section C-1-b-1.

## 2. Discussion and Results

### a. Surface Character (Topography)

All mature\*  $B_4C$  whiskers were found to have common topographical features. Even those whiskers which were individually selected because they appeared to be smooth and shiny when examined by the unaided eye, or under a low power (5X) magnifying lens, proved to have large scale surface features when examined under the optical microscope at a magnification of 875X. The most common topographical feature was a series of flat topped elevations or flat bottomed depressions whose boundaries were observed to have definite angular relationships ( $60^\circ$  or  $120^\circ$ ) with each other and with the whisker axis ( $0^\circ$ ,  $60^\circ$ , or  $120^\circ$ ). The general appearance was one of a

---

\* "Mature" here refers to whiskers thicker than about  $1000\text{\AA}$ . The topographical features of thinner whiskers have not been studied in detail. However even cursory examination (transmission electron microscope) indicates that the very thin whiskers have intrinsic topographical details which in many ways are similar to the details observed on their mature neighbors.

metropolitan skyline in which the buildings and walls are at  $60^\circ$  or  $120^\circ$  with one another. This type of feature is shown in the sketch of Figure 10.

Another common feature was that of relatively long lines or flutes directed parallel to the whisker axis. Close examination showed that these features consisted of step-like formations. The steps formed with risers normal to the surface. Wide-tread planes were parallel to the surface. Figures 11 and 12 show  $B_4C$  whisker regions in which both of the above described features can be observed. Whereas these features were relatively large scale (ca.  $20\mu$  size), it was believed that similar features would be observed on a much smaller scale (ca.  $0.1\mu$ ). This was found to be the case. In Figure 13 is presented the fine surface structural detail as observed on a typical "smooth" and "glossy"  $B_4C$  whisker. Figure 13 is an electron photomicrograph obtained from a surface replica which had been prepared by the technique outlined in Section C-1-b-2. The topographical characteristics which had been observed in the optical photomicrographs of Figures 11 and 12 are directly recognizable, although on a much finer scale, in the more highly magnified (30:1) image of Figure 13. Further examples of the fine surface structure of  $B_4C$  whiskers are shown in Figure 14.

We had previously<sup>(1)</sup> called these surface features "overgrowths". At present, we do not believe this to be appropriate terminology. "Overgrowth" denotes a surface abnormality, a runaway growth. The surface features in the case of  $B_4C$  whiskers are not of the runaway type but are rather the consequence of normal growth, peculiar to this material and to the growth process.

#### b. Origin of Characteristic Topography

Transmission electron microscope examination of many thin  $B_4C$  whiskers provided information concerning the origin of their characteristic topographic detail. A few typical examples will be discussed.

All specimens thin enough for transmission electron microscopy revealed stacking fault contrast effects. The production of stacking faults

is therefore characteristic of the growth process. Diffraction studies, to be described later in Section C2c, showed that the major growth axes of all  $B_4C$  whiskers were parallel to  $\langle h00 \rangle$ , the "a" crystallographic direction (referred to a hexagonal unit cell). All stacking faults were observed to be either parallel to  $\langle h00 \rangle$  or  $120^\circ$  from it, that is in the direction  $\langle 0k0 \rangle$ . The ratio of stacking faults (SF) parallel to  $\langle 0k0 \rangle$ , to stacking faults parallel to  $\langle h00 \rangle$  were found to be:

$$\frac{SF \parallel \langle 0k0 \rangle}{SF \parallel \langle h00 \rangle} = \frac{70 \times 10^4 \text{ cm}^{-1}}{2 \times 10^4 \text{ cm}^{-1}} = \frac{35}{1}.$$

This ratio roughly corresponds to the whisker length to width ratio. Hence, this ratio is related to the growth rates in the two directions. This qualitatively implies; that since the growth rate in the direction  $\langle h00 \rangle$  is about 35 times the rate in the  $\langle 0k0 \rangle$  direction, there exists about 35 times the opportunity for atomic misarrangement to occur in the direction  $\langle h00 \rangle$  as compared to the  $\langle 0k0 \rangle$  direction.

An example of stacking fault configuration is presented in the transmission electron photomicrograph of Figure 15. Note: in all figures in this section, the  $\vec{a}_1$  direction,  $\langle h00 \rangle$ , based on an hexagonal unit cell, is shown parallel to the major whisker growth axis. The enhancement of stacking fault contrasts in Figure 15 is the result of their interaction with strong extinction contours (the dark bands) present in this region. During tilting of the specimen in the electron microscope, the extinction contours are found to move with respect to the specimen whereas the stacking fault details do not. Further examples of characteristic stacking faults are presented in Figures 16 and 17.

The stacking faults parallel to  $\langle 0k0 \rangle$  are readily discernible in the cylindrically bent whisker of Figure 16. Those which are parallel to  $\langle h00 \rangle$  are more difficult to see, some of these are pointed out with small arrows. The dark bands in this figure are extinction contours. It is interesting to apply the simple bent beam formula:

$$\sigma = Et/2R,$$

where

- $\sigma$  = stress, psi
- $E$  = modulus, psi
- $t$  = thickness of beam
- $R$  = radius of curvature of beam

to the  $B_4C$  whisker shown in Figure 16 for the purpose of estimating its tensile strength. Of course, the value for  $\sigma$  obtained by this method is not the ultimate tensile strength. The whisker thickness,  $t$ , was not measured directly, but because of its electron transmission, at 75 KV, it was estimated to be  $500\text{\AA}$  ( $5 \times 10^{-6}$  cm) thick.  $R$  was measured to be  $2.7 \times 10^{-4}$  cm,  $E$  was assumed to be  $65 \times 10^6$  psi. Using these values,  $\sigma$  was calculated to be approximately 600,000 psi.

In Figure 17 is shown a whisker which exhibits doubly reflective symmetry about AA and  $\langle h00 \rangle$  or  $\vec{a}_1$ . It is believed that this growth pattern and others, in which jogs occur in the whisker, result from local inhomogeneities or gradients in the vapor species concentration in the vicinity of the whisker during their growth. We have no evidence that nucleation for growth can occur on a  $B_4C$  whisker. Nucleation can occur only in the vicinity of the substrate. Outcrops or dendritic-type growths are infrequently observed on these whiskers, see Figure 18. This type of growth, we believe, is the result of a fluctuation or anomaly in the vapor species concentration. These growths are always found to occur in an  $\vec{a}$  crystallographic direction.

The initial growth of a  $B_4C$  whisker, from an appropriate nucleation site on the substrate is primarily in the  $\vec{a}_1$ ,  $\langle h00 \rangle$ , crystallographic direction. Growth in the  $\vec{a}_2$ ,  $\langle 0k0 \rangle$ , direction proceeds more slowly (ca. 1/35), in the  $\vec{c}$ ,  $\langle 00l \rangle$ , direction it is still slower (ca. 1/1500). During later stages in whisker development, axial growth slows down and growth in the  $\langle 00l \rangle$  direction becomes dominant. The stacking fault configurations greatly influence later growth. The subsequent incorporation of material in the  $\vec{c}$  direction, influenced by the underlying stacking faults, results in the peculiar and characteristic topographical nature as has been

previously described in Section C-2-a. In Figure 19 is shown a transmission electron photomicrograph of a whisker near maturity. Note the topographical features which are very similar in nature to those found in mature whiskers.

### c. Crystal Character and Whisker Orientation

Electron diffraction and x-ray diffraction examination of individual  $B_4C$  whiskers, when the whiskers were produced by the methods described in this report, showed that they were single crystal. The single crystal character of these whiskers is evidenced by the nature of the diffraction patterns which they yielded. For example, the regular spotty nature of the selected area electron diffraction photograph of Figure 20b, produced from the region of a  $B_4C$  whisker shown in the transmission electron photomicrograph of Figure 20a indicates its single crystal character.

X-ray diffraction analysis revealed that all whiskers were single phase and single crystals of  $B_4C$ . All were found to have their major growth axis parallel to the  $a_1$ , hexagonal unit cell edge (parallel to the  $\langle h00 \rangle$  crystallographic direction).

In Figure 21 is shown an enlarged (2.2X) portion of an indexed 'layer line' x-ray diffraction photograph which was produced from a typical  $B_4C$  whisker. The well defined spots indicate the single crystal character of the specimen. From measurements made on the separation distances of the 'layer-lines',  $y_1$ , and  $y_2$ , on the original diffraction photograph, and from a knowledge of the wavelength,  $\lambda$ , ( $\lambda = 1.5405\text{\AA}$  for  $CuK\alpha_1$ , radiation) and radius,  $R$ , of the cylindrical diffraction camera, the repetition distance,  $p$ , along the axis of the fiber (crystal rotation axis) was obtained from the relationship:

$$p = m \left( 1 + R^2 / y_m^2 \right)^{1/2},$$

where  $m$  = the layer line number,  $m = 0, 1, 2, 3 \dots\dots\dots$

It was thus determined that the repetition distance in all the whiskers examined was  $5.60\text{\AA} \pm 0.02\text{\AA}$ . This distance compares very favorably with the literature<sup>(8)</sup> value for the length of the a-crystallographic edge of the hexagonal unit cell of  $B_4C$ ,  $a_o = 5.61\text{\AA}$ . Hence for these whiskers,

the major whisker axis was parallel to the a-crystallographic direction,  $\langle h00 \rangle$ . Because of alignment problems in the x-ray apparatus due to the small dimensions of the whisker cross sections, the external faces of the  $B_4C$  whiskers have not yet been positively identified. However by making inferences from the morphological character of typical topographic structures on whisker surfaces, from optical and electron photomicrographs, and from the knowledge that the major growth axis is parallel to the 'a' crystallographic direction, one is led to believe that one pair of whisker faces are probably of the  $(00l)$  type while the two others are probably of  $(0kl)$  type. In Figure 10 is shown a schematic representation of the types of topographic features which have been observed on the surfaces of 'a' type whiskers. The  $(00l)$  face is labeled as is the  $(0k0)$  face. Both  $\vec{a}_1$  and  $\vec{a}_2$  of the hexagonal unit cell are parallel to the face of the whisker on which the characteristic structures are shown, the  $(00l)$  face. Since the  $\vec{a}_1$  direction is parallel to the major axis of the whisker then the plane normal to the major axis is a  $(2n, n, 0)$  plane, where  $n = \pm 1, 2, 3, \dots$ . This plane is also indicated in Figure 10. Note: only those planes in which  $n = 0, 3, 6, 9, \dots$  are "reflecting" planes.

In general, one of three quadrilateral cross sections may be expected; (a) rectangle; (b) rhomboid and; (c) trapezoid of which there may be two types. In Figure 22 are shown these typical sections, projected on the  $(2n, n, 0)$  plane of Figure 10. Also indicated on this figure are the angular relations of the quadrilaterals in terms of the Miller indices of the bounding planes.

#### d. Whisker Termini

It was observed that as the whiskers of  $B_4C$  matured that small flags or pennants formed at their tips. A typical example of this type of tip formation is presented in Figure 23. It should be noted in this figure that the whisker is considerably thicker than those seen in the previous transmission electron photomicrographs (Figures 15, 16 and 17). The thickening indicates maturation. In Figure 24-A is shown a field of  $B_4C$

whiskers on their growth mandrel. The view is nearly normal to the mandrel. Here it is to be noted that all whiskers have flagged tips, and the whiskers are nearly all of the same length. In Figure 24B is shown a single whisker and its pennant. The tip of the pennant is out of focus and is directed toward the observer. X-ray diffraction studies proved that (a) the flags were  $B_4C$  and (b) that they were disorganized in that they were not single crystal and (c) their orientation was different than that of the body of the whisker. The tip of the whisker Figure 4-A contains a pennant, however the pennant is directed away from the observer. To be noted in this figure is the highly disorganized nature of the whisker in the vicinity of the flag. Figure 25 is an electron photomicrograph of a replica of a section of a flag. The whisker axis is labeled. This photograph shows the disorganized nature of the flag.

### 3. Mechanism of $B_4C$ Whisker Growth

---

In Figure 26 is shown a composite diagram of the features and mechanisms involved in  $B_4C$  growth. These features have been recognized from optical microscopy, electron microscopy, electron diffraction and x-ray diffraction studies, and have been described in detail in Section C-2. The discussion which follows is based on the features shown in Figure 26.

In the whisker growth region there exists a temperature gradient. The temperature of the substrate, which is heated primarily by conduction, is greater than that of its surroundings. Since the temperature drops off as one proceeds from the substrate the concentration of the vapor species or degree of supersaturation increases in this direction. These facts are shown in the T and C plots on the left of Figure 26. Above a certain critical temperature and conversely below a critical concentration, indicated by the critical plane in Figure 26, whisker growth continues at a sufficiently slow rate, so as to result in a rather regular growth. That is, the atoms which enter into whisker growth have sufficient time, energy and mobility so as to locate themselves in a spatially periodic manner. However due to the concentration gradient, positioning errors can and do occur and stacking faults result. Immediately after nucleation, which is controlled by the



nature of the substrate, thermal environment and impurity (eg. vanadium) concentration, whisker growth proceeds in unique crystallographic directions. Primary growth occurs in the  $\vec{a}_1$ , or  $\langle h00 \rangle$  direction. Secondary growth, which serves to widen the forming bladelet occurs in the  $\vec{a}_2$ , or  $\langle 0k0 \rangle$  direction. The thickness of the forming bladelet in the  $\vec{c}$  or  $\langle 00l \rangle$  direction, remains relatively unchanged during its initial growth. The growth rates of length to width to thickness, during this period, stand in the approximate ratios of, 1:1/35: 1/1500. These growth rates persist until the tip of the bladelet reaches the region of critical supersaturation. At this time, since the concentration of the whisker forming species is too great for the regular positioning of atoms, the growth becomes very much out of step with the remainder of the bladelet and a flag or pennant is formed.

After the flag starts to grow, growth along the major whisker axis stops. From this time on the major growth rate is in the  $\vec{c}$  or  $\langle 00l \rangle$  direction. The bladelet becomes thicker. The stacking fault configuration influences the surface character or topography of the whisker and characteristic topographical features result.

The above description of whisker growth is qualitative. However, it is consistent with the observations which have been made on  $B_4C$  whiskers in various stages of their development.

#### D. COMPOSITE STUDIES

Three matrix materials were used in the composite studies: (1) Fernico "5", (2) PJ 122 epoxy, and (3) Aluminum.

Fernico "5" represents a high temperature material and was selected on the basis of sessile drop results<sup>(1)</sup>. PJ 122 epoxy was chosen because of its ease of handling, tensile strength and wetting ability. Aluminum is extremely useful for structural applications where high strength-to-weight requirements at moderate temperatures are required.

##### 1. Impregnation Techniques

The technique used was essentially that developed by Jakas<sup>(6)</sup> for the formation of composites containing alumina whiskers. A quartz tube is drawn into a capillary whose small diameter lies between 5 to 20 thousandths

of an inch.  $B_4C$  whiskers are placed in the tube through a glass funnel attached to the top of the quartz tube-capillary and are vibrated or tapped into place. Care must be exercised when tapping the tube since the fine tip of the capillary portion is easily broken. Although variation permits better packing of the whiskers, thereby increasing the volume fraction of the resulting composite, failure in the capillary and subsequent loss of the whiskers is risked.

Whisker laden quartz tube-capillaries were subsequently used for all impregnating experiments using both resins and metals.

Resin impregnation is fairly simple. Figure 7 shows a typical arrangement comprised of a ring stand, a whisker laden tube-capillary and a disposable plastic syringe filled with PJ 122 fluid epoxy. Pressure is applied and the epoxy allowed to flow into the whisker bundle. Curing the epoxy is accomplished by oven heating to  $180^{\circ}F$  for 16 hours. The quartz sheath is removed by HF etching, and tensile grips are added to the composite by using a more viscous epoxy which will form a generous bead through surface tension action.

In the case of metal-composite specimens, wires of the matrix metal are also packed into the tube containing the whiskers. The tube is then joined to a long quartz tube, which is then placed in a vacuum apparatus, and the matrix metal is melted by an inductively heated tantalum susceptor. When molten, the metal is forced through the whisker bundle by inert gas pressure. The composite is directionally solidified from the bottom tip to its miniature riser by simultaneous decrease in power and withdrawal of the composite through the hot zone. Figure (8) is a schematic representation of the described apparatus first designed for the infiltration of alumina whisker composites under contract NOw 60-0465d for the Bureau of Naval Weapons<sup>6</sup>.

## 2. Fernico "5" Composites

$B_4C$  exhibits some metallic characteristics and can be wetted by some molten metals as well as being bonded to these metals upon solidification. Metals which wet  $B_4C$ , then, are a good choice for a matrix material with which to bind  $B_4C$  whiskers together in a composite. Previous work has shown that Fernico "5" would be a good high temperature matrix, since it formed a contact angle of  $30^\circ$  with  $B_4C$  which is indicative of good wetting.

The impregnation of  $B_4C$  whisker bundles of Fernico "5" has proved difficult however. Boron is readily dissolved by molten Fernico "5", necessitating the addition of boron to the composite to minimize molten metal attack of the whiskers during impregnation. This was accomplished by placing chunks of bulk  $B_4C$  in the tube below the Fernico "5" wire charge. Thus the molten Fernico "5" should trickle past the boron carbide chunks, reaching the solubility limit for boron before impregnating the  $B_4C$  whisker bundle. When this was attempted, the metal was located further up the tube than where it was originally placed, even though it had been obviously melted. It is postulated that gas evolution during the boron-Fernico "5" dissolution caused the resulting melt to be forced back up the tube and out of the hot zone.

Boron added to the Fernico "5" charge was beneficial in slowing down whisker dissolution while a change in impregnation technique has eliminated the gas evolution problem. It was found that if the system outside the capillary tube was kept under vacuum while the upper portion of the capillary itself was closed off after the pump-down phase, then any evolved gas after the metal was molten travelled toward the capillary instead of blowing molten metal upward as was formerly observed.

The ability to control the above mentioned difficulties has led to a final problem yet to be solved. Fused silica capillaries packed with  $B_4C$  whiskers are used as molds to contain the molten Fernico "5" alloy. The difficulty now lies in forcing the alloy through the packed whisker bundle

which requires a significant pressure. Thus far, due to the pressure required for impregnation and due to the high temperature necessary to keep the Fernico "5" alloy molten, the fused silica capillaries have consistently failed. Techniques which can reinforce the capillaries or resorting to more refractory mold materials are presently being contemplated.

### 3. PJ 122 Epoxy Composites

The highest tensile values of the Epoxy-B<sub>4</sub>C composites reached 24,700 psi for a 10 v/o whisker content, and represented an average tensile value in the whiskers of 193,000 psi. These initial experiments were conducted using the available whiskers. If the yield of whiskers was low for a given run, the product of several growth runs would be combined in order to have a sufficient quantity of whiskers to make one composite test specimen.

During present work, considerable care was taken in selecting only long straight B<sub>4</sub>C whiskers taken from several furnace runs. In one composite specimen (No. 60-SSL-9-56-p3), only whiskers ranging from 1/4 inch in length and upwards were used. Table I presents a compilation of tensile data at room temperature for this composite. A maximum stress of 29,500 psi was supported by the sample. The whisker volume fraction of this particular sample was 5%, representing an average tensile stress on the whiskers of 505,000 psi.

Thus far, it has been possible to produce composites containing a whisker packed density up to 10% by volume. Volume fractions of 30% or more will have to be achieved in order to produce ultra-high-strength composites.

### 4. Aluminum Composites

Aluminum-B<sub>4</sub>C composites were previously fabricated without major difficulty. Whisker bundles were selected without discrimination as to size or shape, and bundles were impregnated with the liquid metal as previously described. The whiskers appeared to be readily wetted by the molten aluminum. There was some difficulty in flowing the molten metal completely through the whisker capillary due to the pressure drop across the bundle and the very small opening in the bottom of the capillary tube.

Table II presents a compilation of the room temperature tensile data of the aluminum-B<sub>4</sub>C composites fabricated during the initial phase of the study. Samples for these tests were formed similarly to the epoxy based specimens (i.e., epoxy beads for grips, etc.).

TABLE I  
TENSILE DATA OF B<sub>4</sub>C - EPOXY SPECIMENS

Test Reference No.	Breaking Load (lbs)	Breaking Stress (psi)	Remarks
60-SSL-9-56-p1	4.4	8800	obvious defect (void)
60-SSL-9-56-p2	4.5	15,200	broke in grip
60-SSL-9-56-p3	6.7	29,500	broke in grip
60-SSL-9-56-p4	8.0	27,000	broke in grip

TABLE II  
TENSILE DATA OF B<sub>4</sub>C - ALUMINUM SPECIMENS

Test Reference No.	Breaking Load (lbs)	Breaking Stress (psi)	Remarks
60-SSL-9-56-A1	3.4	-----	Grip Pulled Out
60-SSL-9-56-A2	3.8	-----	Grip Pulled Out
60-SSL-9-56-A3	5.6	16,200	Broke in Grip
60-SSL-9-56-A4	5.8	29,000	Broke in Grip
60-SSL-9-56-A5	6.45	18,700	Broke in Grip
60-SSL-9-56-A6	4.25	14,400	Broke in Grip

Most later attempts to fabricate aluminum B<sub>4</sub>C composites were not successful. A major problem was the reaction of the molten aluminum with the fused silica capillary molds. It has been observed that a finite time of contact between molten aluminum and B<sub>4</sub>C whiskers was necessary before wetting and impregnation occurs. This is presumably due to a surface reaction between Al and B<sub>4</sub>C whiskers, since wetting does not occur

immediately on direct contact. Thus, a time factor is necessary for the removal of adsorbed gases or films originally present on the surface of the  $B_4C$  whiskers. Because of this phenomena, molten aluminum attack of the fused silica capillaries is substantial if the impregnation time is long. Such techniques as rapid impregnation were unsuccessful, since the Al metal would pass completely through the whisker bundle without reaction or wetting. Techniques such as metallic coatings to promote more rapid wetting were tried in order to minimize this problem, but the results, although somewhat better, were not promising.

In addition to the previously mentioned apparatus, two other ways of performing the impregnations were attempted. One method employed a tube furnace with a thermocouple on the wall of the quartz capillary utilizing both vacuum and pressure techniques to promote infiltration. In addition to these attempts, the capillary was also heated by means of an evacuated quartz tube acting as a susceptor while being heated in air with the capillary kept under argon and under vacuum to effect the infiltration. These methods were essentially unsuccessful in discovering a way to make aluminum -  $B_4C$  whisker composites which would be suitable for a full-scale test program. The few sample composites which were obtained exhibited incomplete wetting, voids, and oxidation. The results of tensile tests on these poor specimens achieved a maximum tensile strength of 14,000 psi at room temperature.

Recently new techniques have been employed to make whisker composites from alumina whiskers<sup>(6)</sup>, and these methods are directly applicable to  $B_4C$  whisker composites technology. Briefly, one technique involves the electroplating and subsequent hot pressing for consolidation with the matrix material being furnished by the plating and the volume fraction of whiskers controlled by plating thickness. Another technique to be studied is the mixing of whiskers with various metal powders and also consolidating the composite by hot pressing techniques in graphite dies. Dies are now being designed and machined to form such composites with both aluminum and Fernico "5" matrices.

#### IV. CONCLUSIONS

A significant contribution to the technology of growing  $B_4C$  whiskers was made. It was discovered that additions of vanadium, molybdenum and niobium to the whisker growing process could greatly enhance the yield and size of individual  $B_4C$  whiskers. These metal powder additions when added to exhausted  $B_4C$  powder (powder which could no longer grow whiskers) showed an equal or better growth of  $B_4C$  whiskers than the best  $B_4C$  bulk powders used to date in the pure vapor method. A patent disclosure has been written to document the discovery of the above described catalysts.

Vanadium chloride gas and vanadium powder additions to the dynamic growth method were also successful in increasing whisker population. However, further work on this method has disclosed a kinetic problem which cannot be easily solved. Provisions must be made to admit unreacted gases to the deposition area without initial heating. Since this is a difficult technical problem without guarantee of success, it was decided to abandon this method.

Geometric studies have also significantly added to  $B_4C$  whisker growth technology. Whisker growing processes, in general, produce only small volumes of usable whiskers for a given run. Thus, additives which can increase whisker yields are most useful. The geometric changes made in the whisker growth chamber have resulted in greater than an order of magnitude increase in whisker yield. A patent docket was also written to document this latest discovery.

The strongest composite to date was an epoxy composite whose tensile strength was 29,500 psi. Since the tensile strength of the epoxy alone is 6,000 psi, an almost 5-fold increase in strength has been achieved. This composite contained only 5 v/o whiskers which corresponds to an average stress of 500,000 psi in the whiskers themselves. The next strongest composite tested was aluminum- $B_4C$ ; it withstood a tensile stress of 29,000 psi. Since the yield stress of pure aluminum at room temperature is about 7,000 psi, a four-fold increase in yield strength had been achieved. This composite contained 10 v/o  $B_4C$  whiskers which corresponds to an average stress in the whiskers of 236,000 psi. Serious technical

difficulties have hampered additional composite fabrication. Mold reactions and whisker packing problems have made the probability of fabricating strong composites difficult. Hot pressing techniques are presently being studied as a means of making strong, high whisker volume fraction composites.

The bend testing of single  $B_4C$  whiskers at high temperatures is progressing. An apparatus has been designed, built, and calibrated using tungsten and glass filaments. Data on  $B_4C$  whiskers should become available shortly.

$B_4C$  whiskers when produced in the manner described in this report are single crystal over their entire length, with the exception of their tips. Their major axes are parallel to the  $\vec{a}_1$ , or  $\langle h00 \rangle$  crystallographic direction. The topographical surface features which these whiskers possess are not the result of a runaway process but rather are characteristic of this material and the growth process. These topographical structures are related to the characteristic stacking fault configurations which the growing whiskers exhibit. The stacking fault density is probably related to variations in the degree of supersaturation of the vapor species in the vicinity of the growing bladelet. It is concluded that the characteristic morphological features may serve a useful purpose in composite formation. They may serve to dovetail the whiskers to the matrix thereby ensuring a better mechanical fit and serve to transfer mechanical loading from the matrix to the whisker, especially in a direction parallel to the major axis of the whiskers.

Nucleation has been found to occur only on the substrate and not on whisker surfaces. Thus nucleation must be greatly influenced by the nature of the substrate and by impurity concentration. In principle, this suggests that the population density and orientation of the resulting whiskers may be controllable through a judicious choice of substrate and through the introduction of suitable impurities.

Whisker growth in the direction of the major whisker axis terminates when the whisker reaches a level in its ambient growth environment in which the degree of vapor supersaturation is too great to support regular or periodic



growth. Therefore, the nature of the vapor phase in terms of its concentration in the vicinity of the growing whisker influences its ultimate length. Thus it is suggested that longer whiskers can be grown by decreasing the concentration gradient in the direction of whisker growth. This can be accomplished by carefully controlling the temperature gradient in this region, through the introduction of properly shaped (finned, etc.) mandrels, etc.

## ACKNOWLEDGEMENTS

Acknowledgement is given to Messrs. W. Laskow, C. Miglionico, T. Harris, R. Jakas and J. Chorné for their valuable assistance in this program.

## References

1. A. Gatti, et al, "The Synthesis of Boron Carbide Filaments", NASw -670 Final Report. July 10, 1964.
2. H. E. Robsin and P. W. Gilles, "The High Temperature Vaporization Properties of Boron Carbide and The Heat of Sublimation of Boron", J. Phys. Chem. Vol 68, 1964 , 983-985.
3. A. E. Newkirk, Private Communication.
4. G. L. Pearson et al, "Deformation and Fracture of Small Silicon Specimens", Ceta Met 5, 1957 181-191.
5. H. D. Conway, "The Large Deflections of Single Supported Beams", Phil. Mag. 38 1947 905-11.
6. Sutton et al, "Development of Composite Structural Material for High Temperature Applications", Quarterly Report 1-18, Navy Bu Weps Contract NOw 60-0465d.
7. R. L. Mehan et al, "Evaluation of Sapphire Wool and Its Incorporation into Composites of High Strength" GE Co., Contract No. AF 33(61 )-1696, BPSN NR 64-6899-7351-735103, 3rd Quarterly Progress Report, Feb. 15, 1965.
8. ASTM X-Ray diffraction data card 12-212.

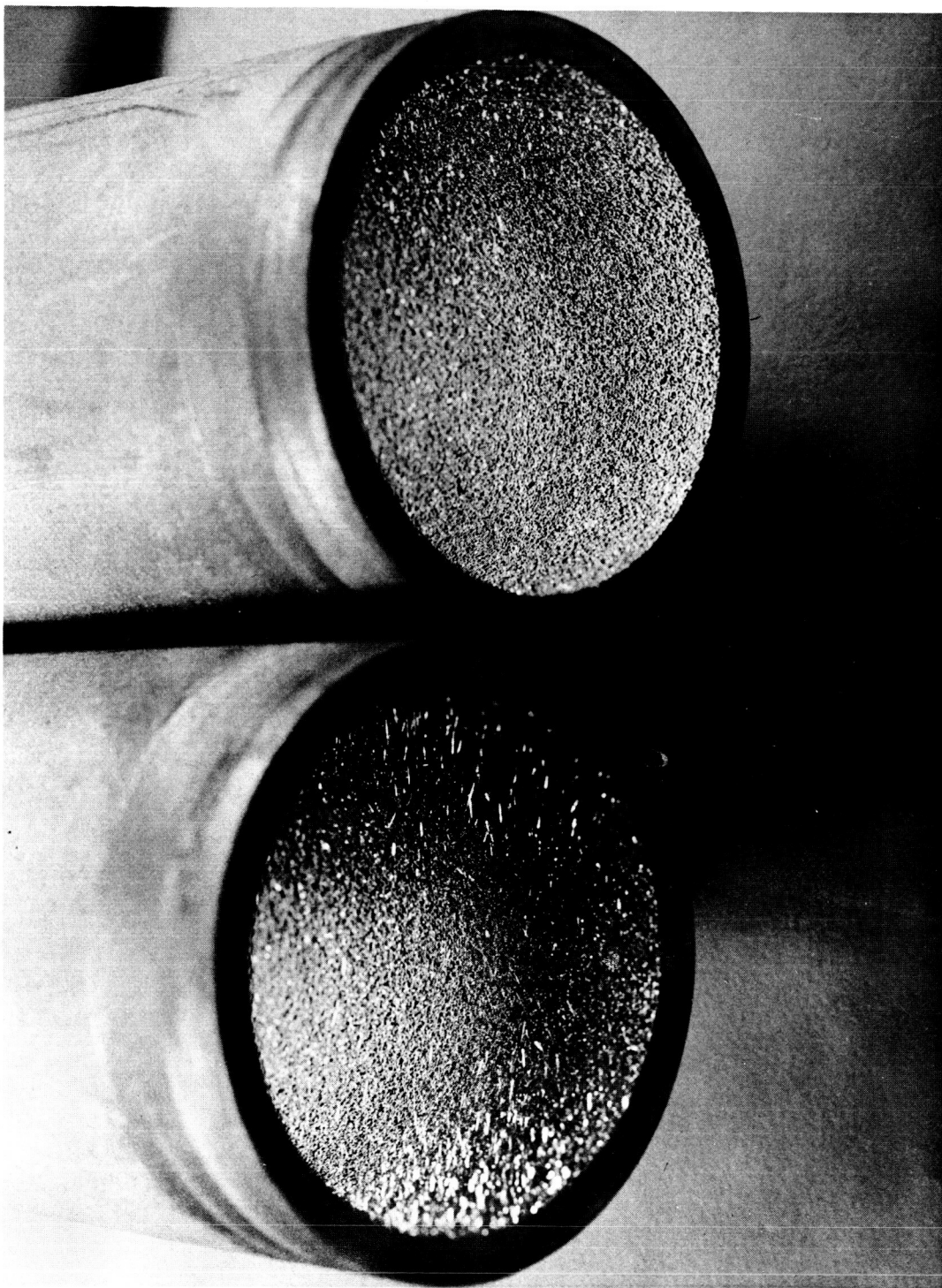
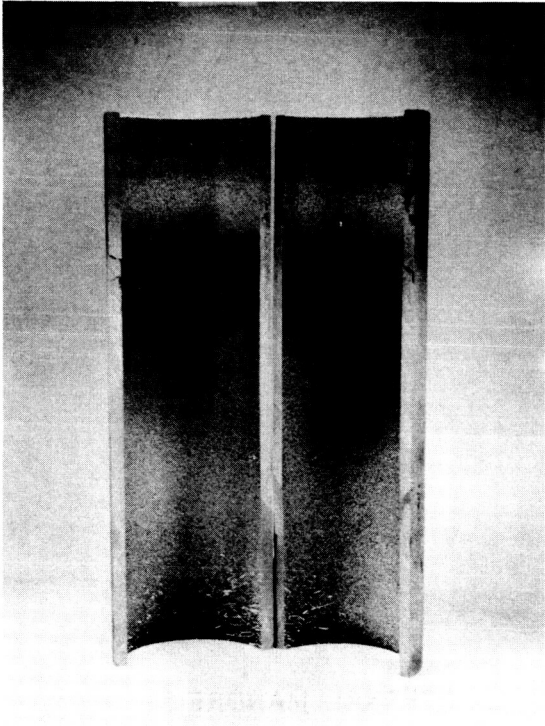


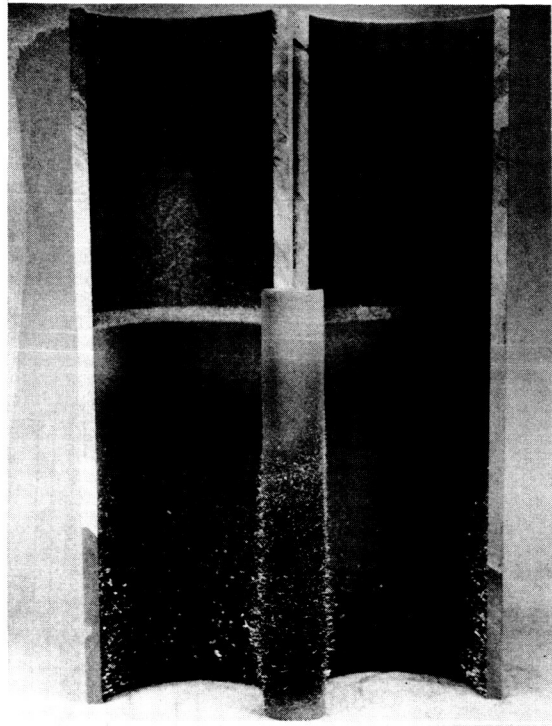
Figure 1. Photograph Showing the Effect of Vanadium on the Growth of  $B_4C$  Whiskers. Of the Two Growth Tubes Shown, Vanadium was Added to the Charge Only in the Furnace Containing the Lower Tube



Figure 2. Photograph Showing Additional Mandrel Added to Top of "Lazy Susan" Tray (About 1/3 Size)

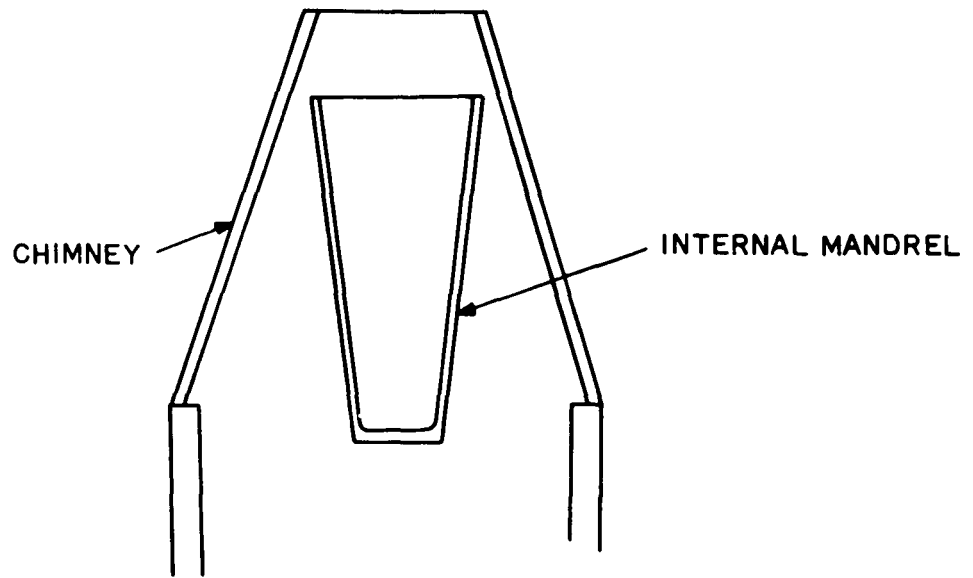


(a)

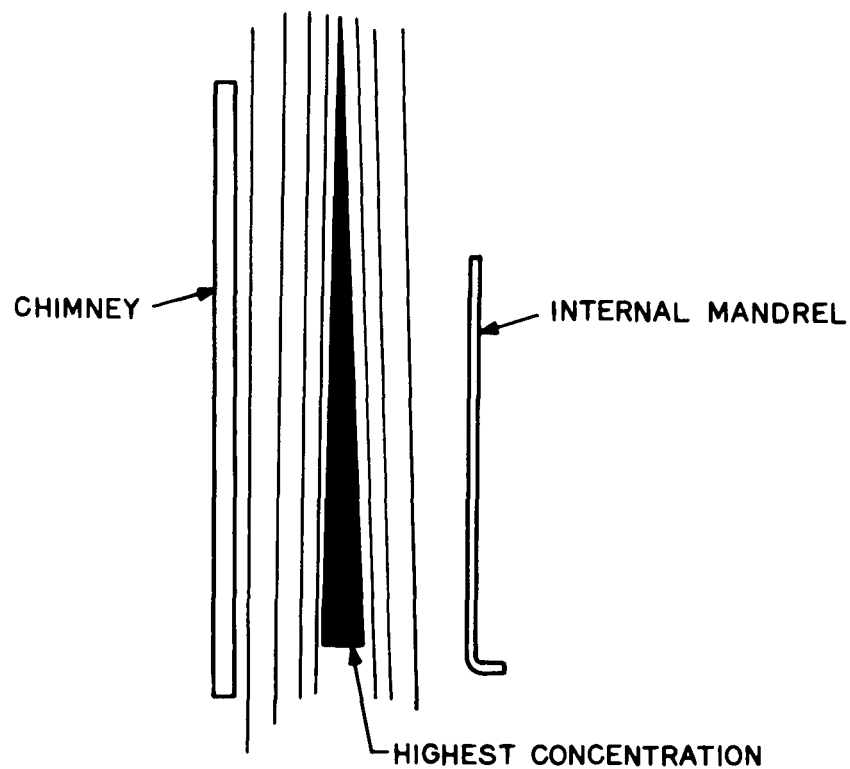


(b)

Figure 3. (a) Typical Run Before the Internal Mandrel and Baffle Additions (About 1/2 Size)  
(b) Typical Run After Mandrel and Baffle Additions (About 1/2 Size)



(a)



(b)

Figure 4. a. Schematic Representation of Proposed Conical Chimney Design  
 b. Schematic Representation of Hypothesized Vapor Gradient

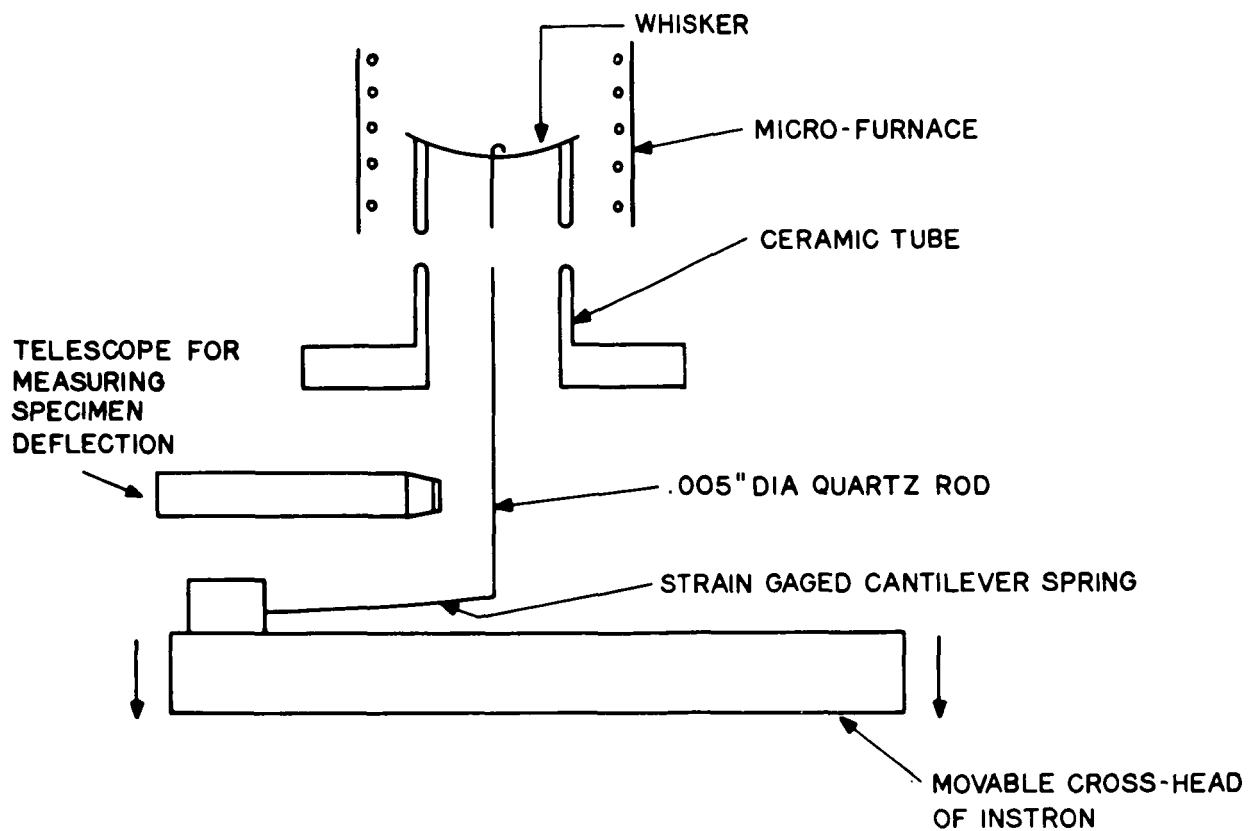


Figure 5. Schematic Design of Whisker Bend-Test Apparatus



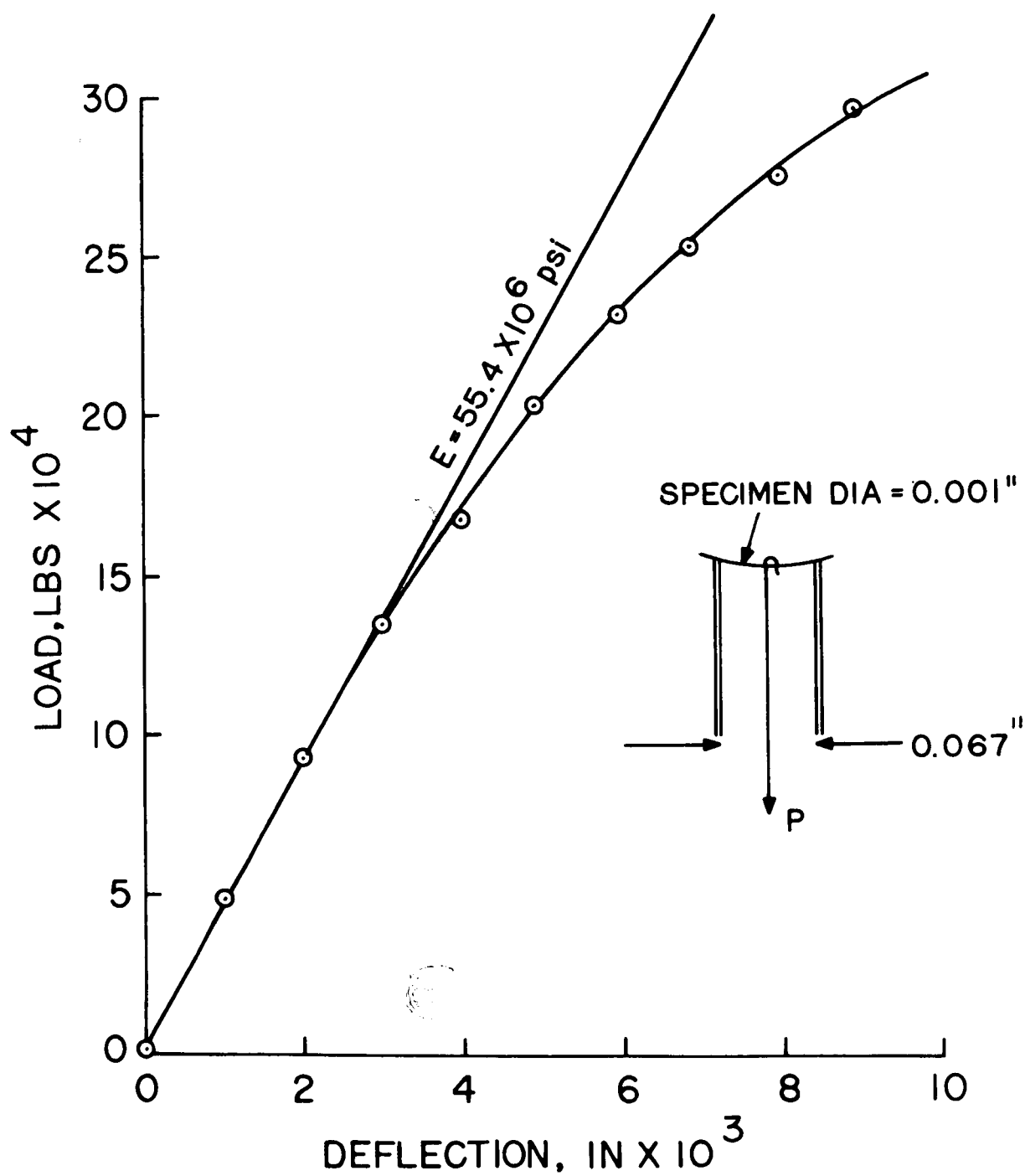


Figure 6. Load-Deflection Calibration Curve of .001 Diameter Tungsten Wire at Room Temperature

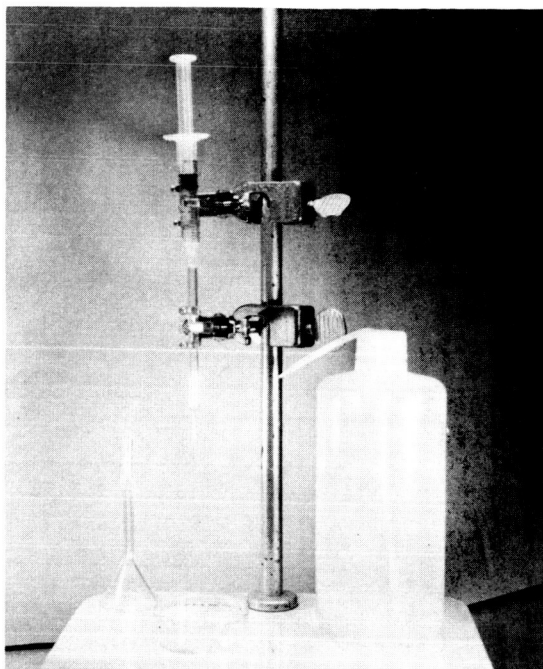


Figure 7. Photograph of 1/3 Size of Tube-Capillary and Arrangement for Epoxy Impregnation of  $B_4C$  Whisker Bundles

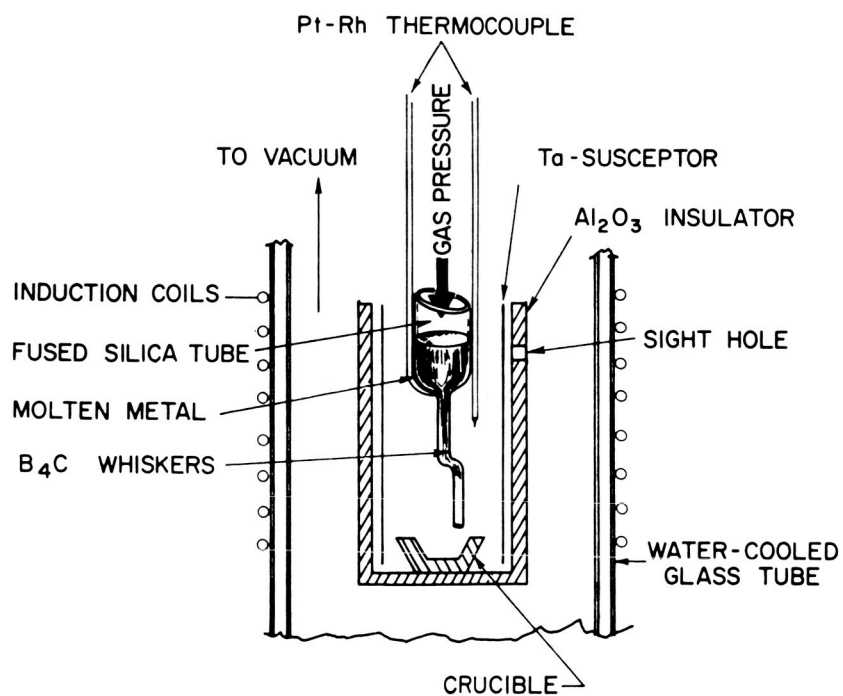


Figure 8. Schematic Diagram of Furnace for Fabricating  $B_4C$ -Metal Composites by Pneumatic Pressure Technique

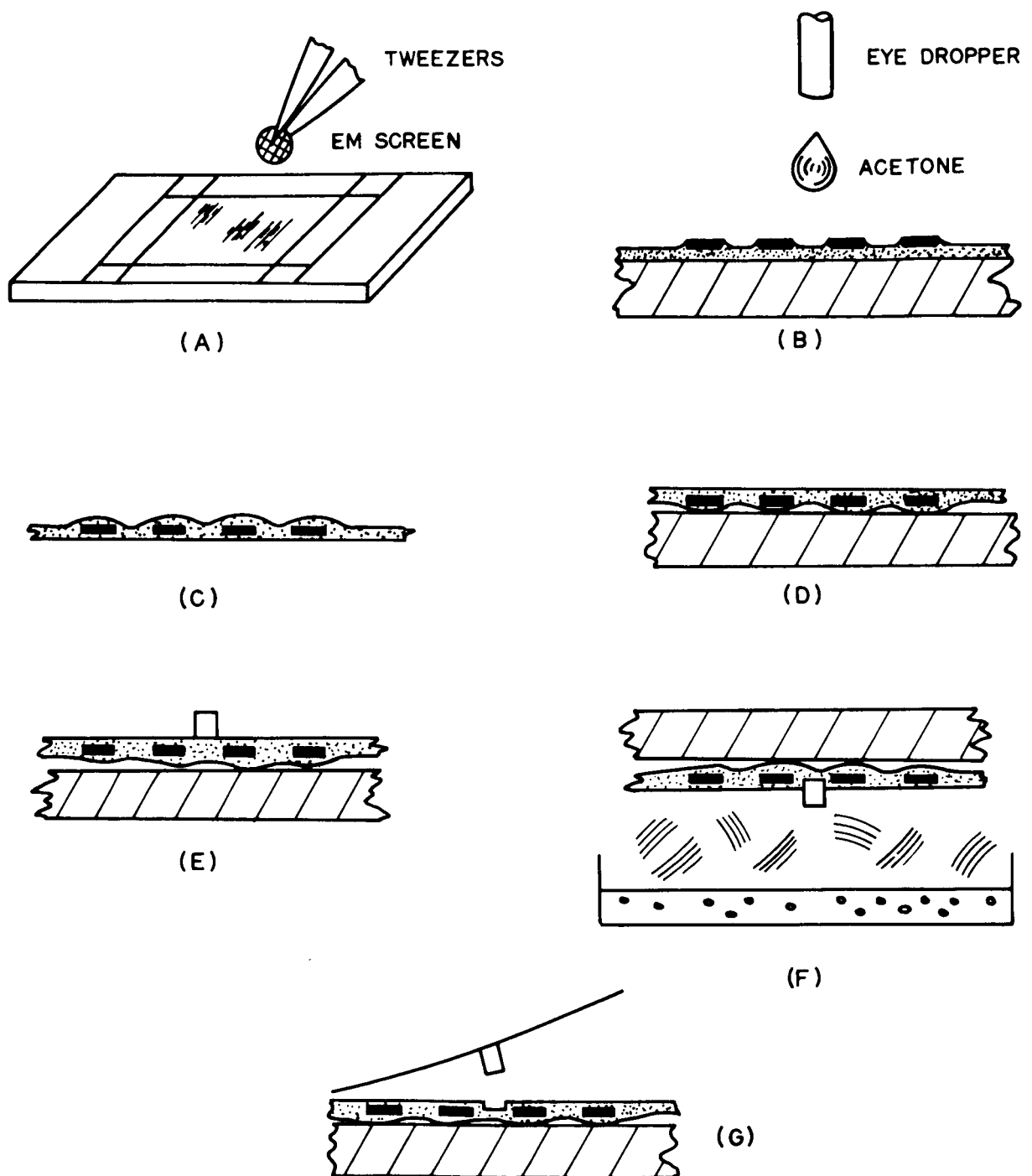
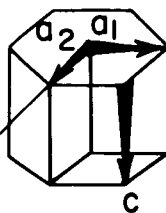


Figure 9. Preparation of Primary Cellulose Acetate Replica of a Small Object

# HEXAGONAL UNIT CELL OF $B_4C$



$$a_1 = a_2 = 5.61 \text{ \AA}$$

$$c = 12.07 \text{ \AA}$$

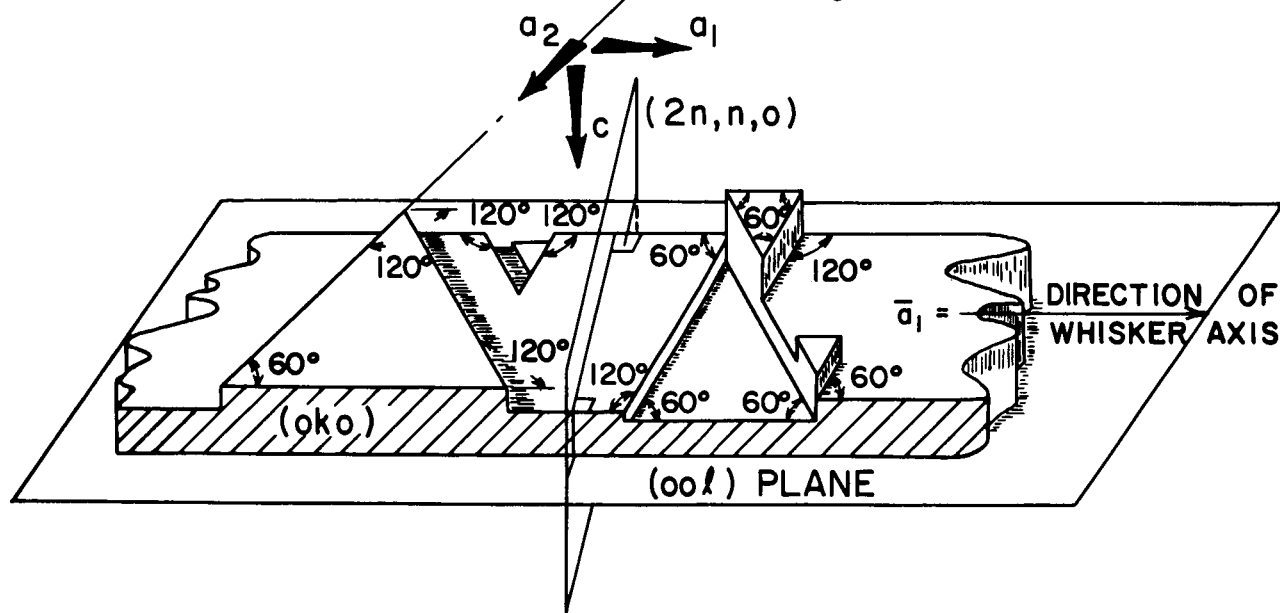
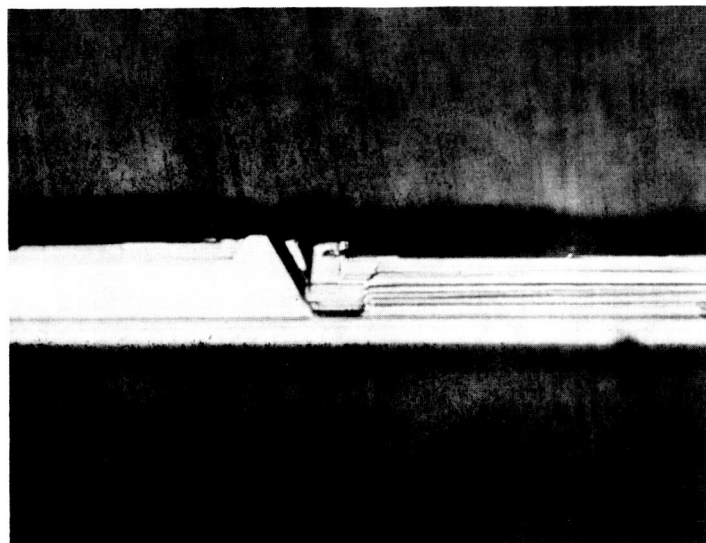
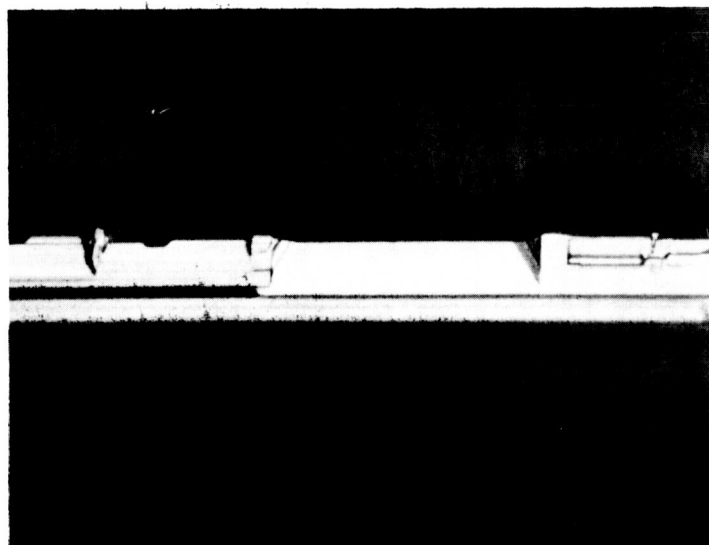


Figure 10. Schematic Representation of Typical Topographical Details Observed on  $B_4C$  Whiskers



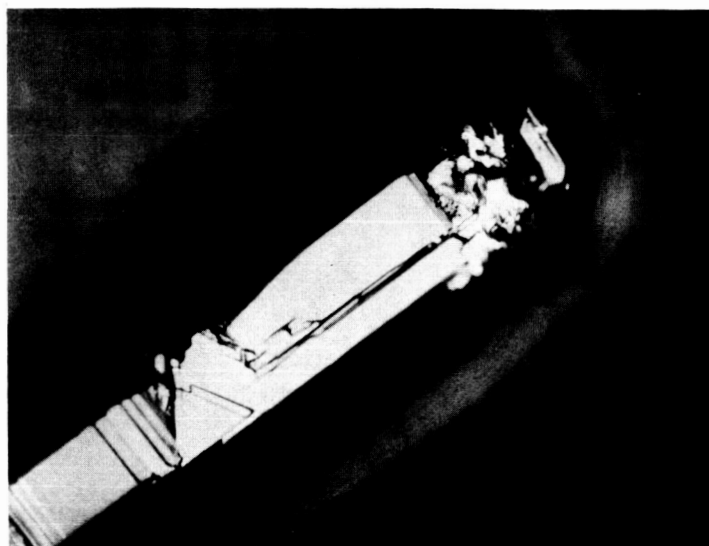
(A)



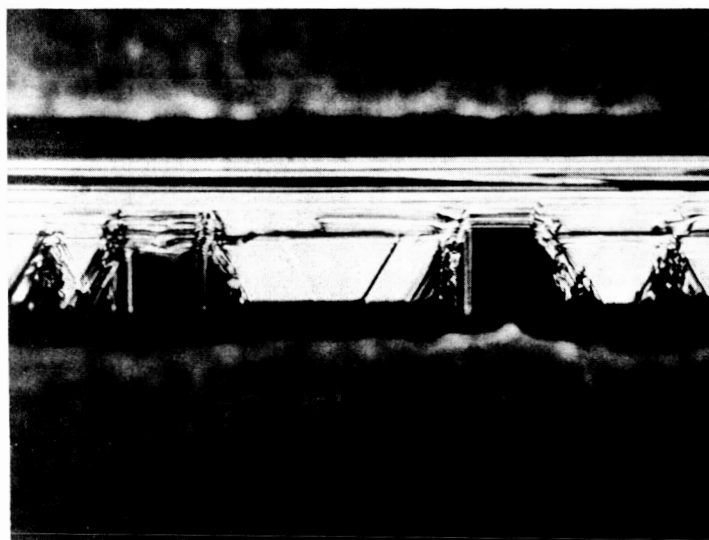
(B)

50 $\mu$

Figure 11. B<sub>4</sub>C Whisker Surface Details. Magnification = 875X



(A)



(B)

50  $\mu$

Figure 12. B<sub>4</sub>C Whisker Surface Details. A. Note Large Scale Imperfections Near Whisker Tip. Magnification = 875X

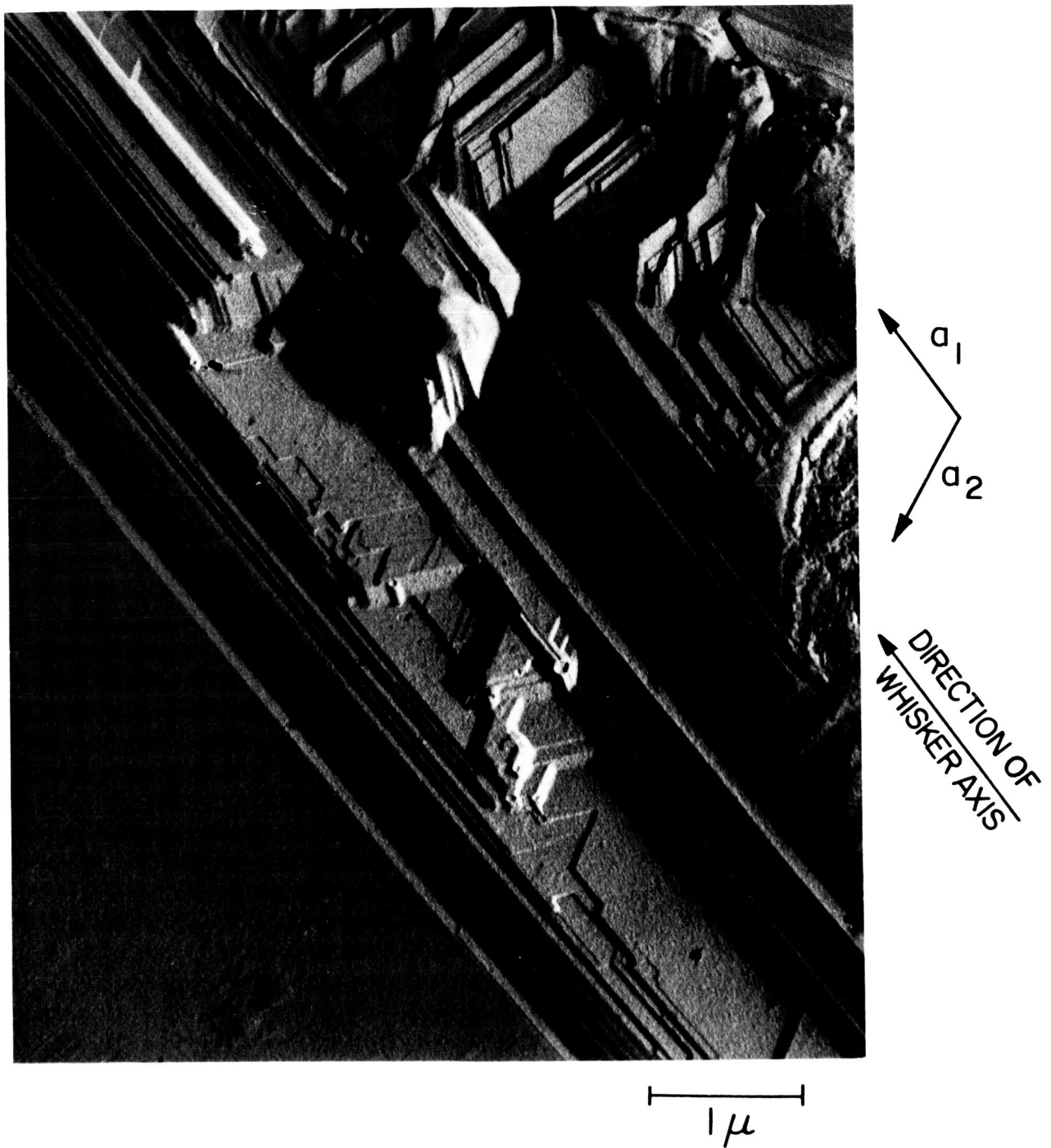


Figure 13. Electron Photomicrograph of a Replicated Portion of a "Smooth"  $B_4C$  Whisker. Magnification = 25,200X

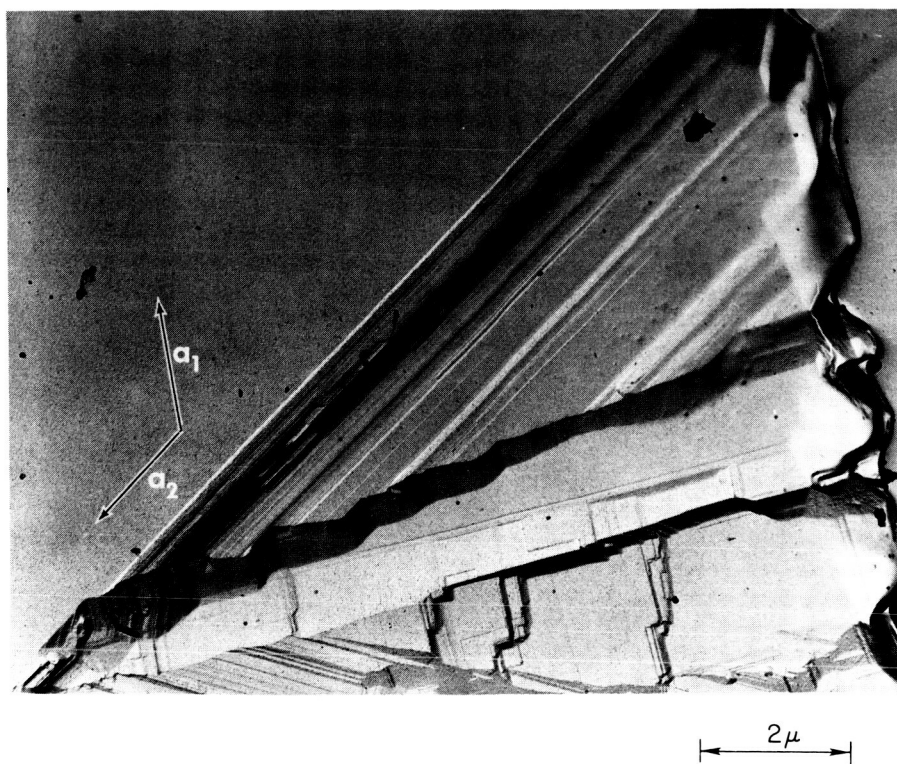
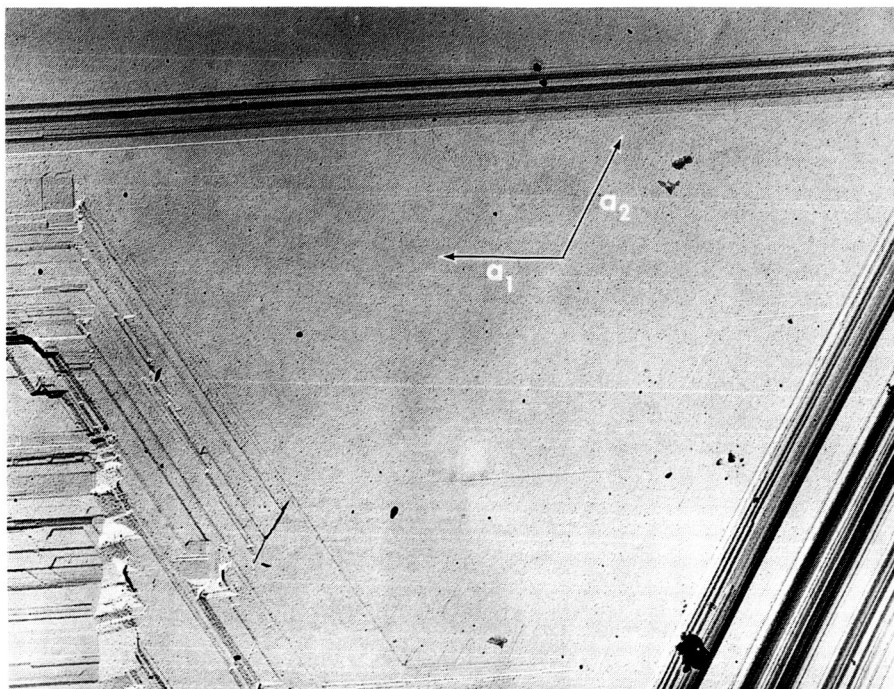


Figure 14. Electron Photomicrographs of Portions of "Smooth"  $B_4C$  Whiskers. Magnification = 20,000X





Figure 15. Transmission Electron Photomicrograph of a Thin  $B_4C$  Whisker. Note the Stacking Fault Configuration Parallel to  $\vec{a}_1$  and  $\vec{a}_2$ . Magnification = 69,000X

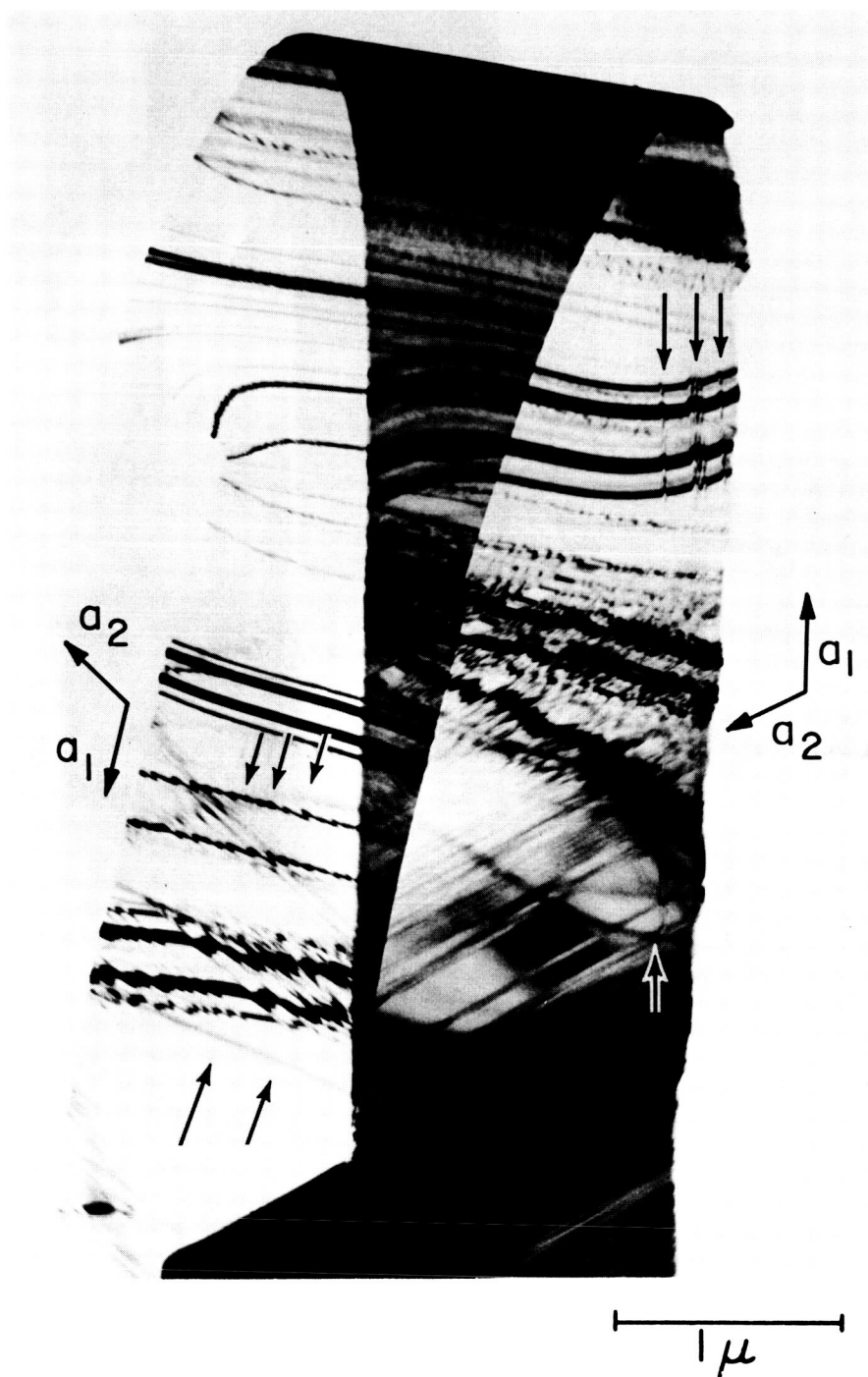


Figure 16. Transmission Electron Photomicrograph of a Thin Cylindrically Bent B<sub>4</sub>C Whisker. Note Stacking Fault Configuration Parallel to  $\vec{a}_1$  (arrows) and Parallel to  $\vec{a}_2$ . Magnification = 30,000X

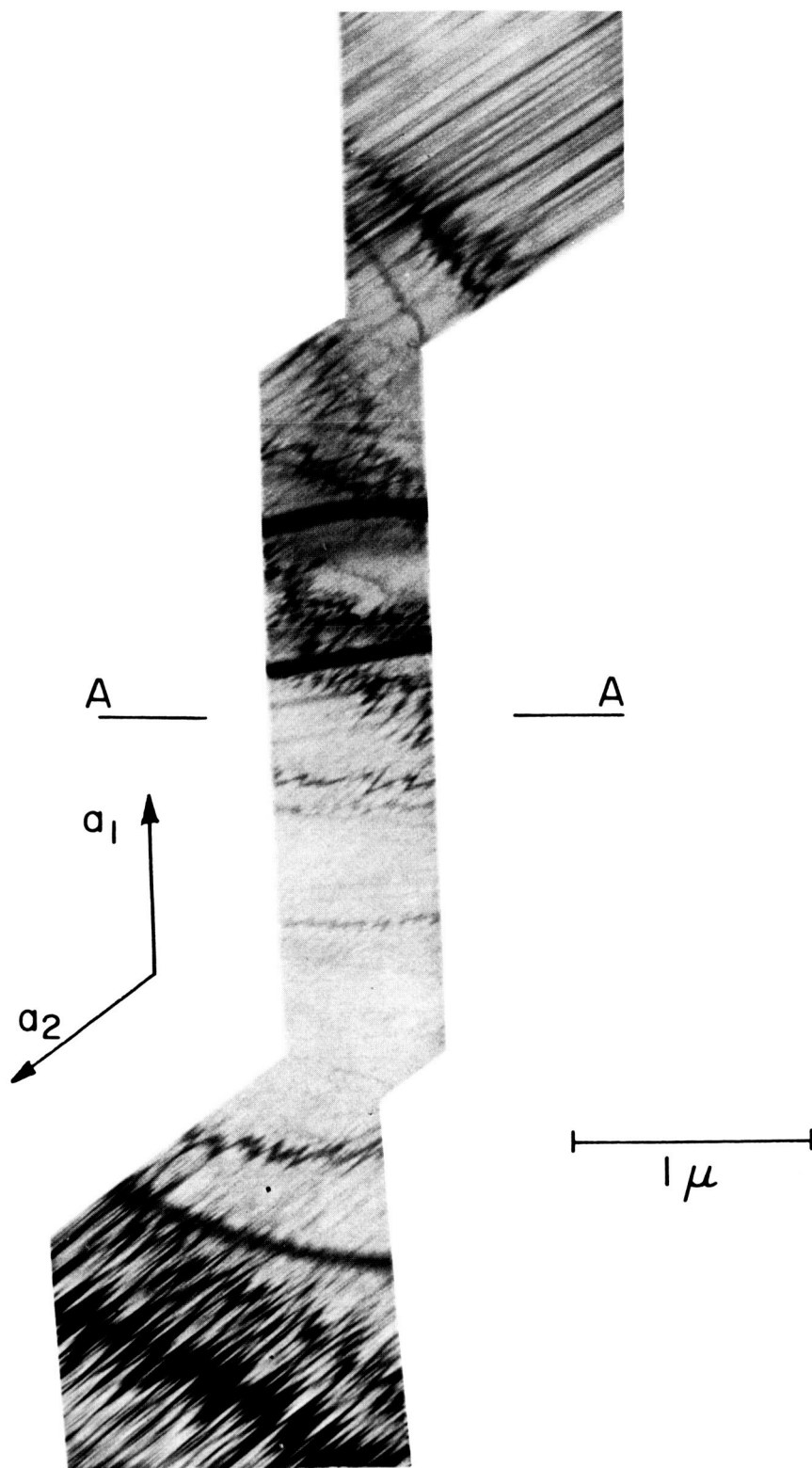
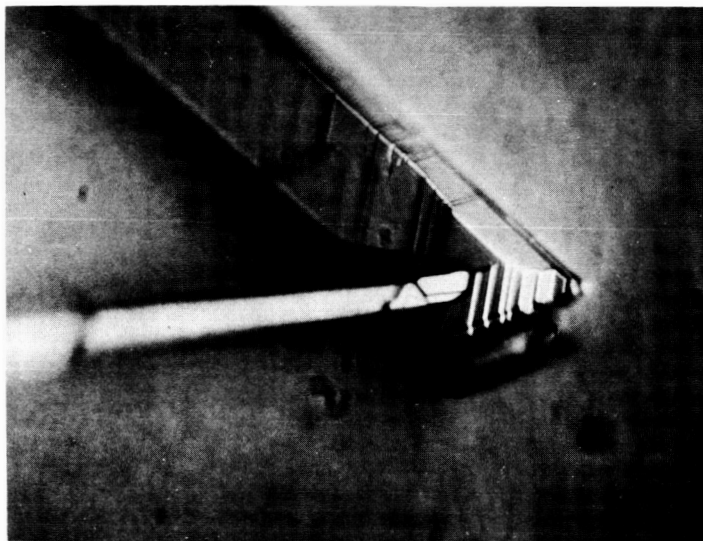


Figure 17. Transmission Electron Photomicrograph of a Thin  $B_4C$  Whisker. Note Symmetry About AA and  $\vec{a}_1$ . Magnification = 36,000X



50  $\mu$

Figure 18. Typical, but Rare, Outgrowths from  $B_4C$  Whiskers.  
Magnification = 875X

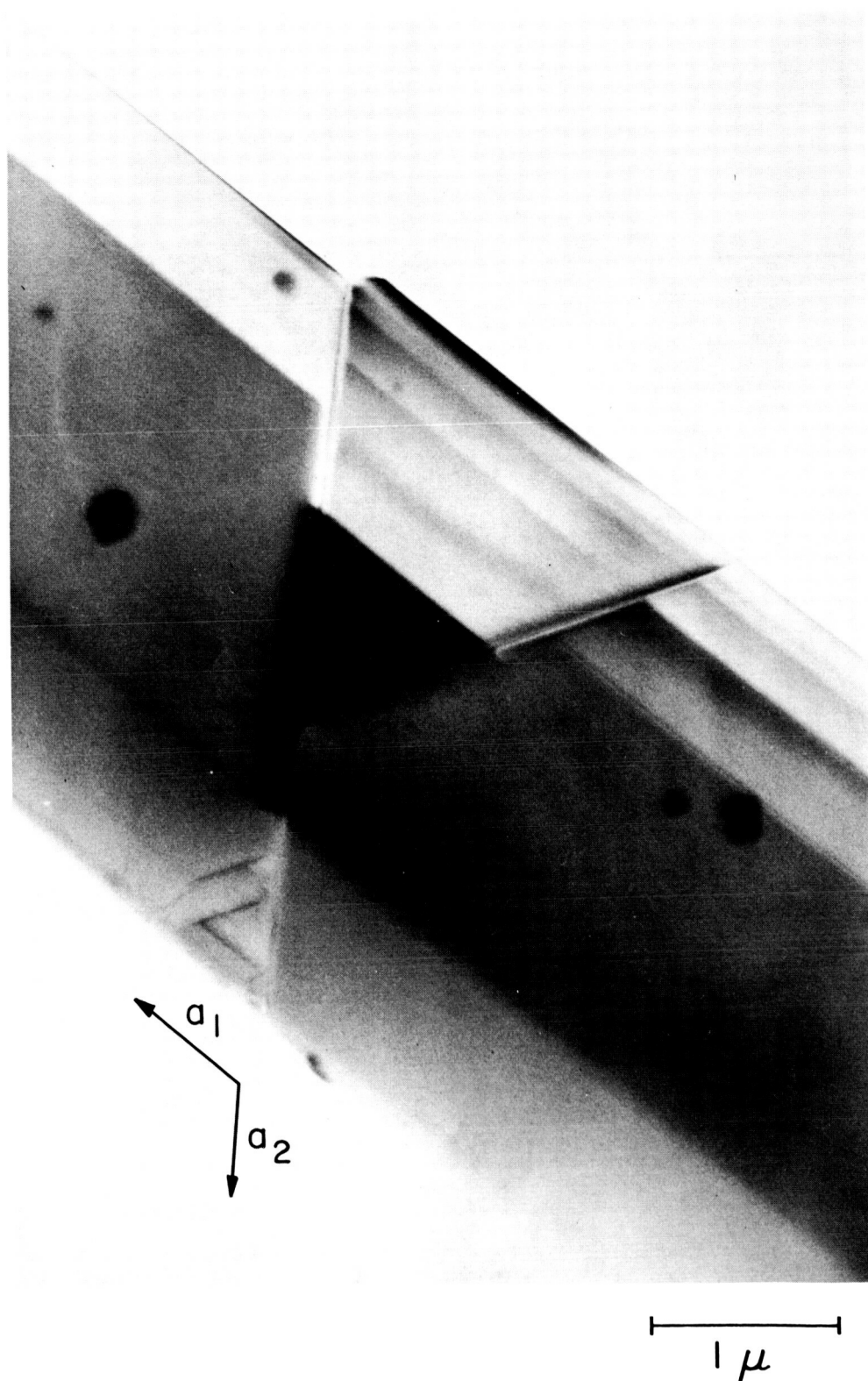
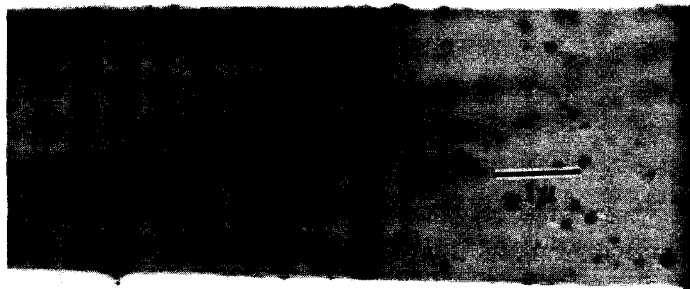


Figure 19. Transmission Electron Photomicrograph of a B<sub>4</sub>C Whisker During a Late Stage of Development. Magnification = 30,000X



(a)

Magnification 11,000 X



(b)

Figure 20. Transmission Electron Photomicrograph of a Region of a Typical B<sub>4</sub>C Whisker (a) and an Electron Diffraction Pattern of the Same Region (b)

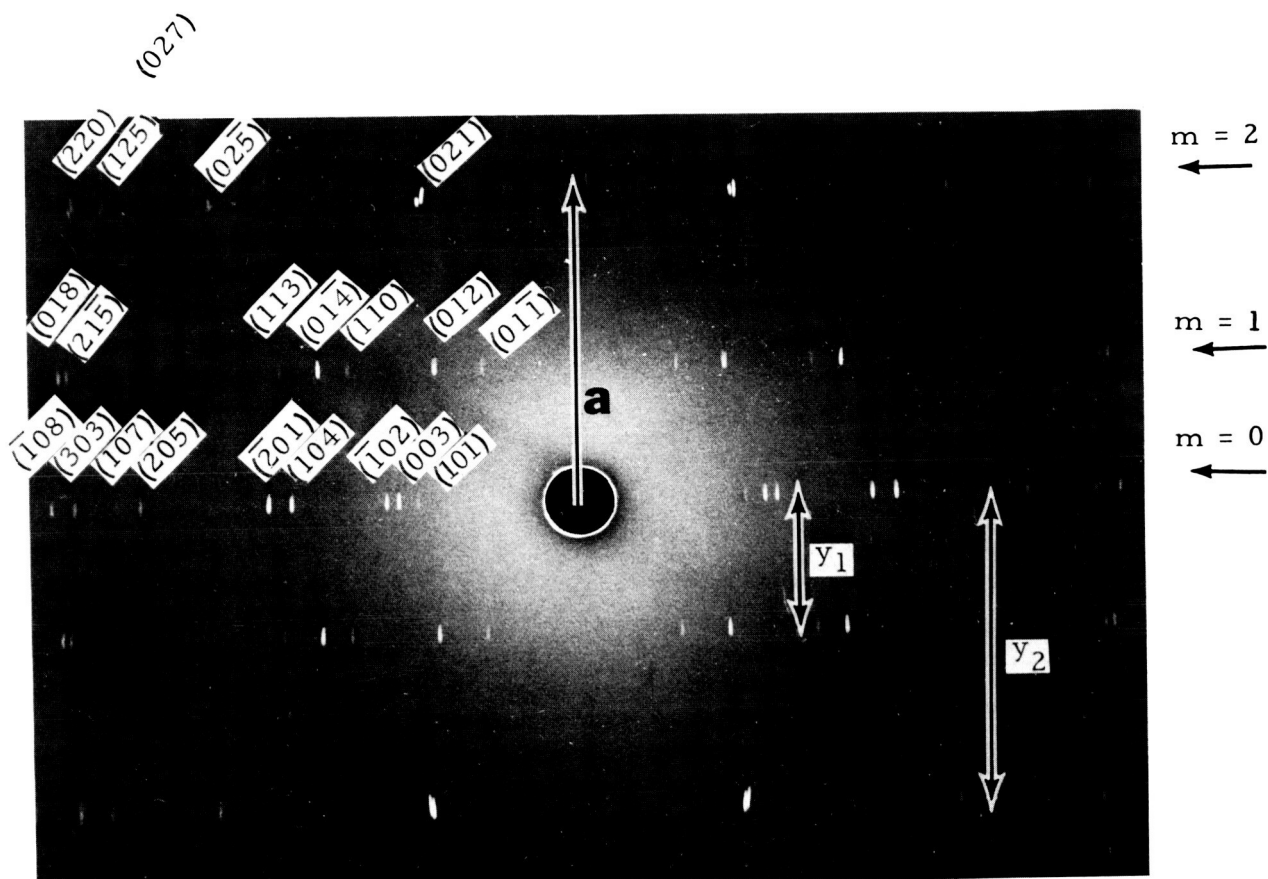
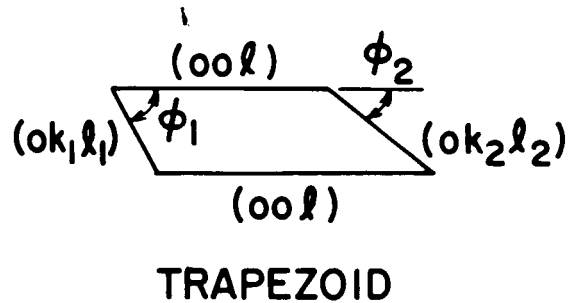
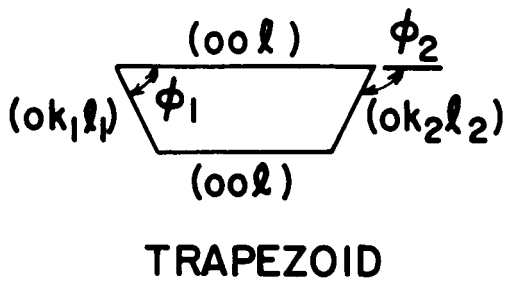
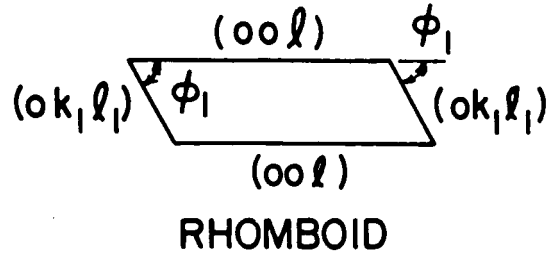
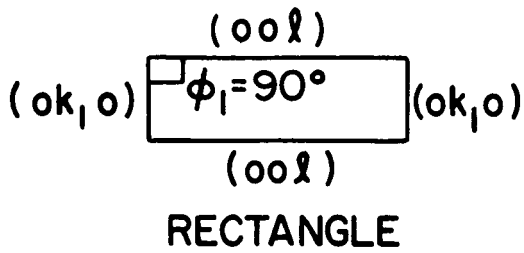


Figure 21. X-ray Diffraction "Layer Line" Photograph (2.2X) of a Typical ("a" Type) by  $B_4C$  Whisker. The Whisker Axis was Parallel to  $\vec{a}$ .



$$\phi_1 = \tan^{-1} \left( \frac{2}{\sqrt{3}} \frac{c}{a} \right) \frac{k_1}{l_1} = \tan^{-1} 2.4843 \frac{k_1}{l_1}$$

$$\phi_2 = \tan^{-1} \left( \frac{2}{\sqrt{3}} \frac{c}{a} \right) \frac{k_2}{l_2} = \tan^{-1} 2.4843 \frac{k_2}{l_2}$$

Figure 22. Predicted Quadrilateral Whisker Cross Sections



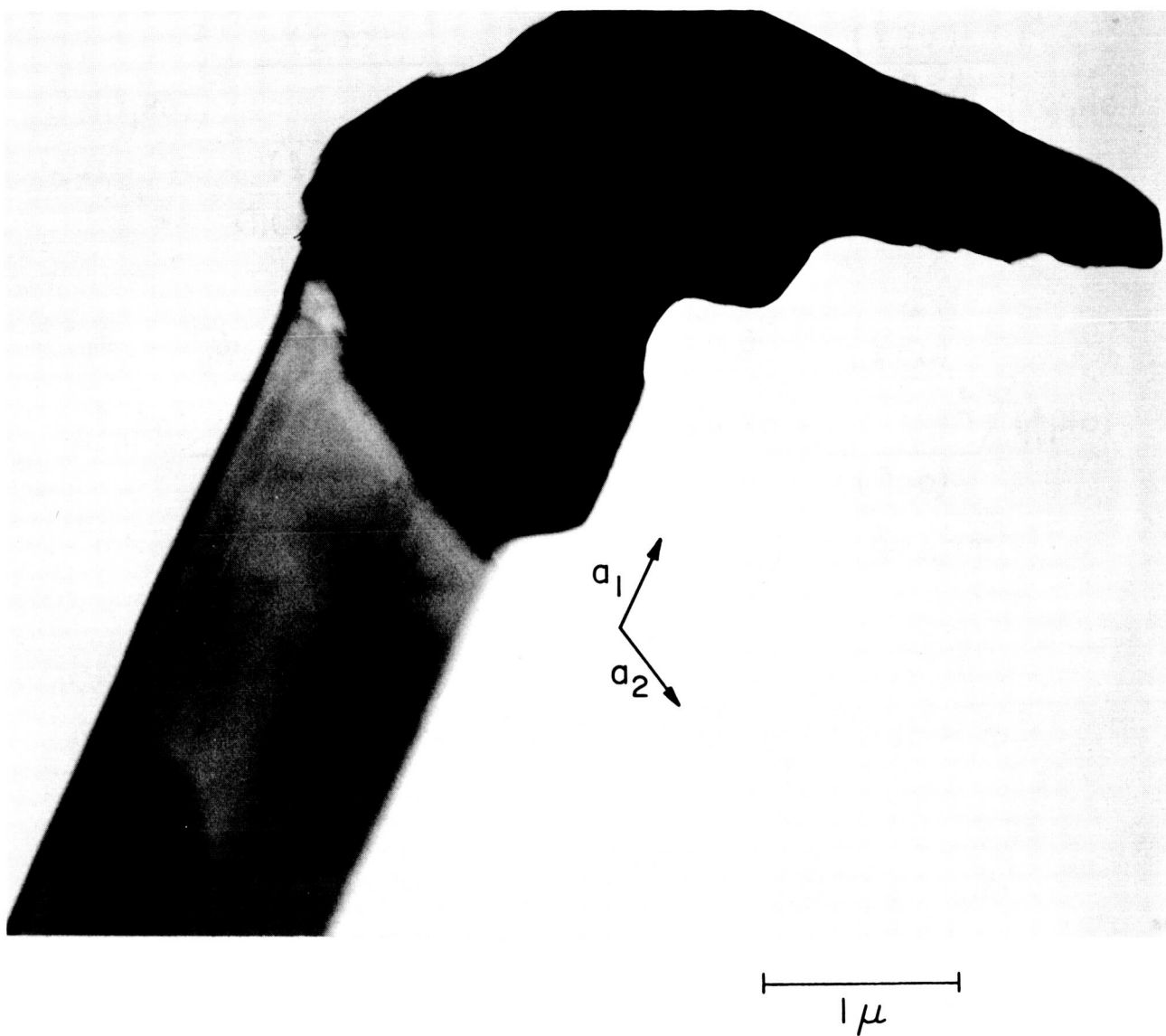
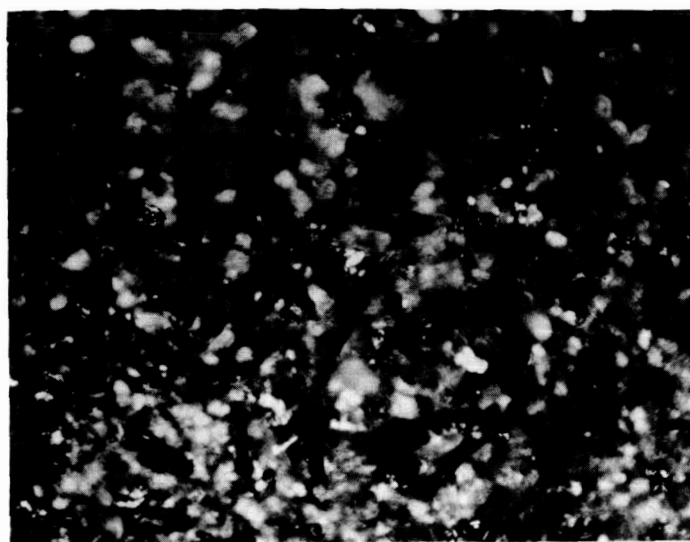
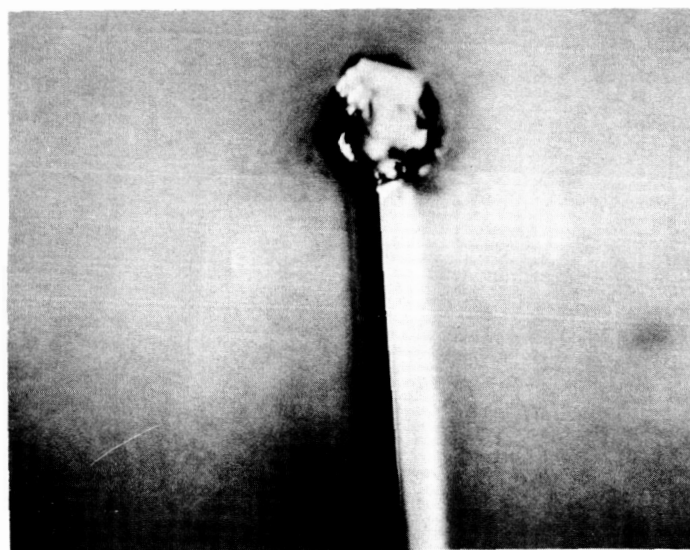


Figure 23. Flag or Pennant Tip of Maturing B<sub>4</sub>C Whisker Transmission Electron Photomicrograph. Magnification = 30,400X



(A)

100 $\mu$



(B)

50 $\mu$

Figure 24. A. Field of  $B_4C$  Whiskers, on Their Growth Mandrel, Showing Flags or Pennants on Their Tips, Magnification = 163X  
 B. Pennanted Tip of a  $B_4C$  Whisker. Pennant is Directed Toward Observer. Magnification = 875X

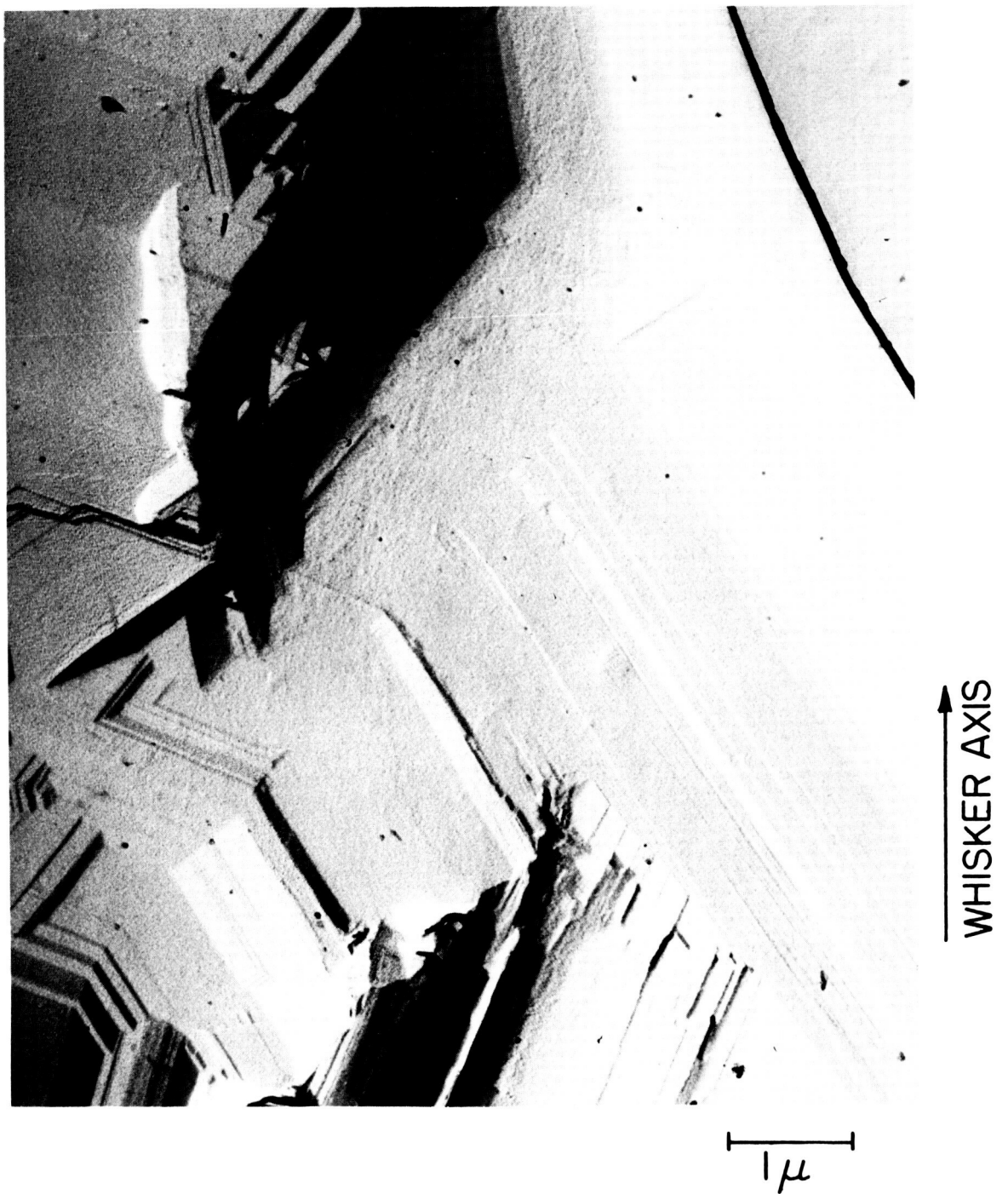


Figure 25. Flag Region of B<sub>4</sub>C Whisker Electron Photomicrograph of Replica. Magnification = 20,000X

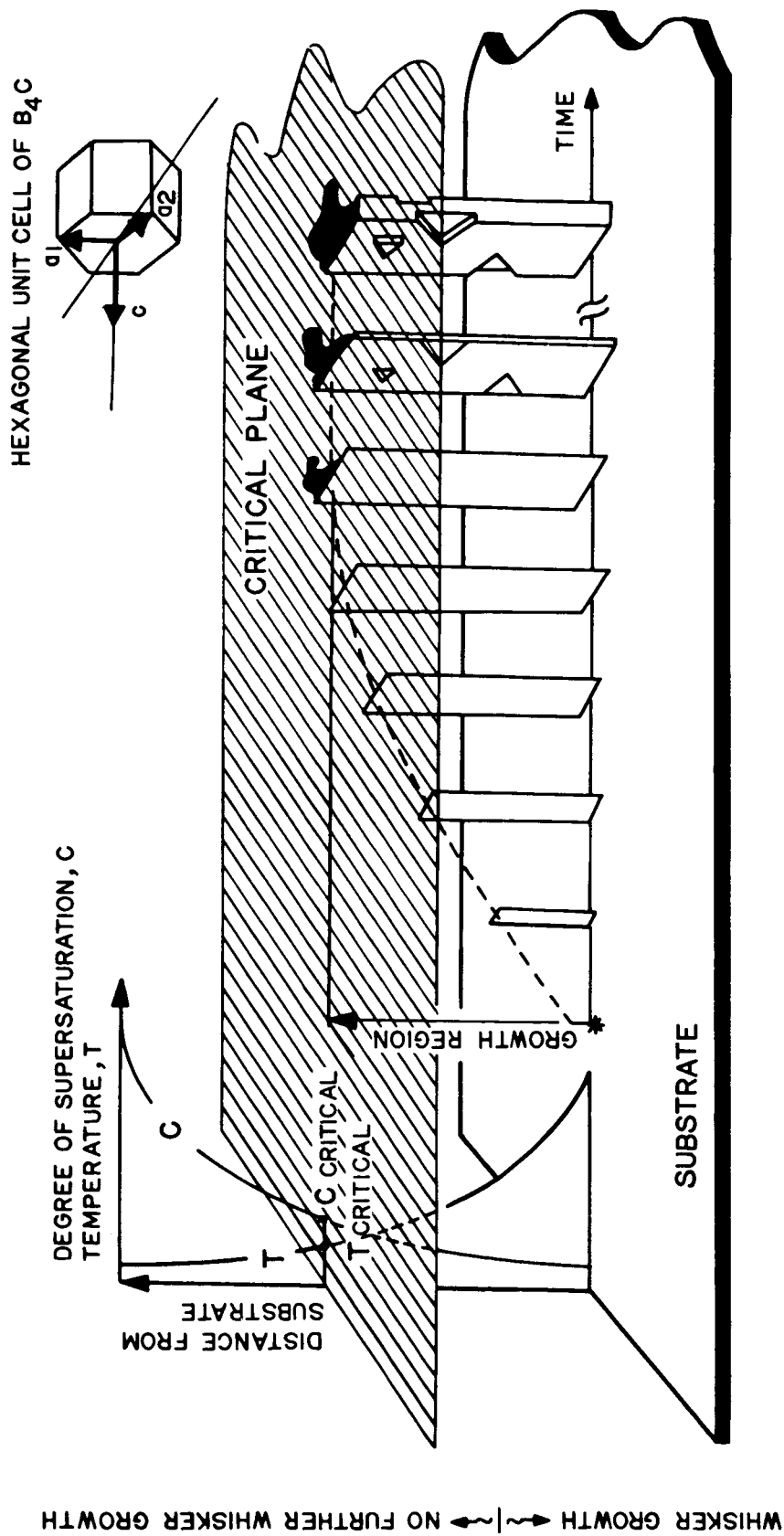


Figure 26. Schematic Representation of Factors Involved in  $B_4C$  Whisker Growth Process